NASA CONTRACTOR REPORT

DYNAMIC RESPONSE OF STRUCTURAL ELEMENTS EXPOSED TO SONIC BOOMS

by David H. Cheng and Jacques E. Benveniste

Prepared by
CITY COLLEGE OF NEW YORK
New York, N. Y.
for Langley Research Center

NATIONAL AERONAUTICS AND SPACE ADMINISTRATION • WASHINGTON, D. C. • MARCH 1969

DYNAMIC RESPONSE OF STRUCTURAL ELEMENTS EXPOSED TO SONIC BOOMS

By David H. Cheng and Jacques E. Benveniste

Prepared under Grant No. NGR 33-013-011 by
CITY COLLEGE OF NEW YORK
New York, N.Y.

for Langley Research Center

NATIONAL AERONAUTICS AND SPACE ADMINISTRATION

For sale by the Clearinghouse for Federal Scientific and Technical Information
Springfield, Virginia 22151 – CFSTI price $3.00

ABSTRACT

This report summarizes recent analytical results on the subject of dynamic response of structural elements exposed to sonic booms. The structural elements of interest are uniform beams and plates with various boundary conditions. The disturbances are represented by a variety of boom signatures which approximate those obtained from field measurements.

Responses of structural elements to a unit impulse and to a unit force moving at a constant velocity are first obtained. This enables a comparison to be made of the relative dynamic effects of an N-shaped pressure pulse and an N-shaped traveling wave on a simple structure. It is followed by a study on the effects of boundary restraints using an N-shaped pressure pulse.

Based on the results due to such idealized boom signatures as sine pulse, half-cosine pulse, triangular pulse, N-shaped pulse, and N-shaped pulse with spikes, two simplified methods in evaluating the boom effects on structural elements are proposed: One requires only the knowledge of the peak pressure and the other, the positive impulse. Neither requires the specification of the exact shape of the boom signature.

The above methods are very simple to use, and are applicable to structural elements which are always in contact with the supports. Considerable higher dynamic effects can be expected in cases in which the structural element is loosely bound to supports and may rattle in the wake of boom disturbances. As an illustration, a uniform rattling beam is considered in the Appendix.

TABLE OF CONTENTS

		Page
1	Introduction	1
2	Nomenclature	2
3	Dynamic Response of Structural Elements to Boom Signatures of Arbitrary Shape	4
4	Structural Response to N-shaped Pressure Pulse and to N-shaped Traveling Wave	7
5	The Effects of Boundary Restraints	9
6	Structural Response to Various Idealized Boom Signatures	11
7	Effects of Damping	14
8	A Simplified Approach to Evaluating Effects of Sonic Booms	15
9	Concluding Remarks	17
	Bibliography	18
	Appendix	20

1. INTRODUCTION

The purpose of this report is to summarize some recent analytical results on the subject of dynamic response of structural elements exposed to sonic boom shock waves. The subject matter, though important, constitutes only one aspect of a problem of much wider scope.[1]*

The structural element under consideration may be a component of a building such as rafters, studs, window panes, wall panels, etc. and which may be typified as a uniform beam or a uniform rectangular plate with various boundary restraints. It is understood that the dynamic effect is primarily due to the direct application of the shock wave and the secondary effect arising from the interaction of the element with the rest of the building can be neglected. On the other hand, the element is arbitrarily oriented in relation to the direction of propagation of the disturbance. Hence, in limiting cases, it may be subjected either to a pressure wave traveling across its span or to a pressure pulse.

The wave shape of the shock waves in far-field has been found [2] to be describable by a capital N if the wave is propagated through a homogeneous atmosphere. Reliable methods [3] are now available to predict adequately the wave shape and magnitude for steady supersonic flight taking into consideration such factors as aircraft configuration, altitude, ground reflection, Mach number and reference pressure in an ideal atmosphere, etc. However, there will be complications when the aircraft is not in a steady flight [4] and the atmospheric condition deviates, as it always does, from the assumed isothermal hydrostatic condition. [5] [6] Although progress in delineating the various effects has been made analytically, it is understandable that, at the present, more reliable data can only be obtained from measurements in field. [7] [8] [9] A representative group of measured boom signatures is reproduced in Figure 1. It should be pointed out that all these signatures may be present for a steady, level flight at localities spaced along the ground track only a few hundred feet apart. It is not unreasonable therefore to assume that a structural element may be subjected to any one of these disturbances at one time or another.

The dynamic response of uniform beams and rectangular plates having simply-supported and clamped-clamped boundary conditions and subjected to an N-shaped pressure pulse was first investigated by Cheng** and followed by a study of simply-supported beams and plates subjected to a traveling N-shaped pressure wave. The treatment was later extended to traveling pressure waves of arbitrary shape. [10] A similar treatment has appeared [11] recently together with some laboratory experimental verifications. Damped dynamic

---

* Number in square parentheses refer to the Bibliography

** Unpublished work submitted by David H. Cheng, City College of the City University of New York, prepared during temporary assignment at NASA, Langley Research Center.

response of structural elements exposed to a group of typical sonic boom disturbances was obtained by an analog computer which facilitated construction of a realistic envelope for the maximum response. Based on the envelope, some simplified methods were devised. [12] To study the effect of rattling in the wake of sonic boom of a structural element which is not initially in direct contact with supports, an analytical solution was obtained for a beam. [13] In related developments, using lumped structural models, one study was made on the effect of the near-field and far-field sonic booms [14] and another on the dynamic response of a display window including the effect of coupling with the roof. [15] Currently, an effort is being made [9] in correlating the cause and effect through field measurements.

In what follows, essential results obtained in some of the above-mentioned analytical studies will be presented in a compact form, but in a manner consistent with the aim of presenting a realistic solution to a rather complex problem. The results will be given in terms of a dimensionless quantity called the dynamic amplification factor (hereafter DAF) and defined as the ratio of the maximum dynamic moment to the static moment due to the uniform peak pressure developed at the same point in the structure. The DAF is expressible in terms of another dimensionless quantity known as the period ratio. The latter is defined as the ratio of period (or duration) of disturbance to that of the structural element. Finally, two simplified methods will be presented: one requires only the knowledge of the peak pressure and the other, the positive impulse. Neither requires the specification of the exact wave shape of the shock wave. The limitations of these methods will be discussed including a treatment in the Appendix on the response of a beam loosely bound to supports exposed to a typical sonic boom.

2. NOMENCLATURE

Unless otherwise specified in the text the following nomenclature will be used:

a	side of a square plate
a'	half gap
A	a'/ℓ
A_b, A_p	Dynamic amplification factor (DAF) for beam and plate, respectively
C_n	Fourier coefficient
DAF	Ratio of maximum dynamic moment and static moment at a point of structural element
EI	Flexural rigidity of beam

$EI/12(1-\nu^2)$	Flexural rigidity of plate
$H(t)$	Unit step function, =0 if $t < 0$; = 1 otherwise
I_o	Positive impulse (positive area) of sonic boom signature
k	Spring constant of a single oscillator
$K(K_b, K_p)$	Dynamic moment coefficient (for beam and square plate, respectively)
K'	$EI/S\ell^3$
ℓ	Span length of beam
L	Linear differential operator, $= \frac{EI}{\mu}\frac{\partial^4}{\partial x^4}$ for beam, $= \frac{EI\ \nabla^4}{12(1-\nu^2)}$ for plate
m, n	Integers
p_o	Peak pressure of sonic boom
p_n, p_{mn}	Natural frequency of beam and plate, respectively
$P(t)$	Forcing function
q	Phase indicator
r	Aspect ratio of rectangular plate
R, R_1	Period ratio (τ/natural period of structure) in any mode and in fundamental mode, respectively
R_i'	τ/T_1'
R_d	$p_o l^3/EI$
$\tilde{s}$	Rise time ratio, t_1/τ
s, f	Superscripts denoting simply-supported and free-free boundary condition, respectively
S	Spring constant
t_1	Rise time for triangular pulse
t_c	Critical time
$\tilde{t}$	Dimensionless time ratio t/τ
T_i'	Fundamental period of free-free beam
T_n	Time function
v	Constant velocity of traveling wave
∇^4	Biharmonic operator
α, β	Coefficients defining spike
δ	Dirac delta function

φ_n, φ_{mn}	Dynamic amplification function (daf) for beam and plate, respectively
φ_1', φ_{11}'	daf in the fundamental mode of beam and plate, respectively, due to N-shaped traveling wave
$\overline{\varphi}$	Asymptotic value of daf
ν	Poisson's ratio
μ	Mass per unit length (unit area) for beam (plate).
τ	Period or duration of disturbance
ζ	Damping factor

3. DYNAMIC RESPONSE OF STRUCTURAL ELEMENTS TO BOOM SIGNATURES OF ARBITRARY SHAPE

A number of typical boom signatures recorded in the field are shown in Figure 1. To facilitate analyses, these signatures can be idealized into mathematically describable shapes, although it is obviously more appropriate to consider the boom signature as arbitrary in shape. The structural elements may be uniform beams and plates with various boundary conditions. They are commonly found in buildings in the form of rafters, studs, window panes, etc. In this section, we shall first obtain the general form of response of structural elements of any boundary condition, to certain unit disturbances with a view toward generalization later to boom signature of any shape. It will be followed by more specific treatment of structural elements having specific boundary conditions and subjected to specific boom signatures. The aim is to find the most critical combination of these conditions, boundary as well as loading.

Let the coordinate system be selected so that the x-y plane coincides with the neutral surface of the structural element with the z-axis in the direction of deflection. The governing equation may be written as:

$$L z + \ddot{z} = \frac{1}{\mu} P \tag{1}$$

where L is a self-adjoint linear differential operator whose domain consists of twice differentiable functions satisfying appropriate boundary conditions. For a beam, z and P are functions of x and t, and L stands for $EI/\mu \; \partial^4/\partial x^4$. For a plate, z and P are functions of x, y and t, and L is $EI \nabla^4/12(1-\nu^2)\mu$.

For a beam and a plate, there is an obvious analogy in the responses to a given disturbance. It is therefore sufficient to consider only the beam response in detail with the understanding that the results for the plate can be

obtained simply by analogy. Taking the origin of coordinates at the left support of the beam, the finite transforms of z and P take the following forms:

$$\bar{z}(n,t) = \int_0^{\ell} z(x,t)\, z_n(x)\, dx$$
$$\bar{P}(n,t) = \int_0^{\ell} P(x,t)\, z_n(x)\, dx \qquad (2)$$

where z_n is the n-th normalized eigenfunction having the property:

$$\int_0^{\ell} z_n^2(x)\, dx = 1 \quad , \qquad (3)$$

and ℓ is the beam span. Equation (1) can thus be transformed into an ordinary differential equations as follows:

$$p_n^2\, \bar{z}(n,t) + \ddot{\bar{z}}(n,t) = \frac{1}{\mu}\, \bar{P}(n,t) \qquad (4)$$

where p_n^2 is the n-th eigenvalue. For zero initial condition, the solution to Eq.(4) is:

$$\bar{z}(n,t) = \frac{1}{\mu p_n} \int_0^t \bar{P}(n,t) \sin p_n (t-t')\, dt' \qquad (5)$$

and, by the inverse transformation, one gets:

$$z(x,t) = \sum_{n=1}^{\infty} \frac{z_n(x)}{\mu\, p_n} \int_0^t \bar{P}(n,t) \sin p_n (t-t')\, dt' \qquad (6)$$

Analogous to Eq. (6), the response of a plate can be written as:

$$z(x,y,t) = \sum_{m=1}^{\infty} \sum_{n=1}^{\infty} \frac{z_{mn}(x)}{\mu\, p_{mn}} \int_0^t \bar{P}(m,n,t) \sin p_{mn} (t-t')\, dt' \qquad (7)$$

Now the beam response to two kinds of unit disturbances which are illustrated in Figure 2 may be considered:

(A) Uniformly Distributed Unit Impulse

The forcing function is:

$$P(x,t) = \delta(t) \tag{8}$$

whose finite transform is:

$$\overline{P}(n,t) = \int_o^{\ell} z_n(x)\,\delta(t)\,dx = C_n\,\delta(t) \tag{9}$$

substituting into Eq. (6), one gets:

$$z(x,t) = \sum_{n=1}^{\infty} \frac{C_n\, z_n(x)}{\mu\, p_n} \sin p_n t \tag{10}$$

(B) Unit Force Moving at a Constant Velocity (v)

The forcing function is:

$$P(x,t) = \delta(x - vt)\, H(\frac{\ell}{v} - t) \tag{11}$$

where $\delta(x-vt)$ is a distribution x with v and t as parameters. Its finite transform is:

$$\overline{p}(n,t) = z_n(vt)\, H(\frac{\ell}{v} - t) \tag{12}$$

Substituting into Eq. (6), there results:

$$z(x,t) = \sum_{n=1}^{\infty} \frac{z_n(x)}{\mu\, p_n} \int_o^t z_n(vt') \sin p_n(t-t')\, H(\frac{\ell}{v} - t')\, dt' \tag{13}$$

Equations (10) and (13) may be considered as two basic solutions for the dynamic response of a beam exposed to sonic boom disturbances. [10] If the boom disturbance is in the form of a pressure pulse, using Eq.(10), the corresponding beam response can be obtained by integration. Similarly, if the disturbance is a moving wave, the beam response can again be obtained by integration by the use of Eq.(13). In both instances, the shape of the pressure pulse or of the moving wave can be arbitrary as long as it is describable analytically.

4. STRUCTURAL RESPONSE TO N-SHAPED PRESSURE PULSE AND TO N-SHAPED TRAVELING WAVE [10]

In order to ascertain the relative severity of response of a structure subjected to a pressure pulse and to a moving wave, it is convenient to consider a typical shape in the form of a capital N in conjunction with a simple beam. As shown in Figure 3, the N-shaped signature can be described as:

$$P(\xi) = p_o(1 - 2\xi/\tau)\, H(\tau - \xi) \tag{14}$$

It is noted that as far as the beam is concerned, the loading is a pressure pulse when the wave normal $\bar{n}$ is in the direction of deflection; and a moving wave when $\bar{n}$ is parallel to its span. The eigenvalue and the normalized eigenfunction of a simply-supported beam are, respectively:

$$\begin{aligned} p_n^2 &= (n\pi/\ell)^4\, EI/\mu \\ z_n(x) &= \sqrt{2/\ell}\, \sin n\pi x/\ell \end{aligned} \tag{15}$$

where n is chosen to be an odd integer corresponding to symmetrical modes of oscillations. In the case of a pressure pulse, only symmetrical modes are excited. In the case of a moving wave, the maximum dynamic stress occurs around the midspan. Again only the symmetrical modes are of interest.

The beam response to a pressure pulse now can be obtained as follows. First substitute Eq.(15) into Eq.(10), then multiply the resulting equation by Eq.(14), the response results by simply integrating with respect to ξ. The maximum response is obtained as the sum of the maxima of all modes. Since the static moment at the midspan is $p_o\ell^2/8$, the DAF for the beam takes the following form:

$$A_b = 1.03 \sum_{n=\text{odd}}^{\infty} \left| \frac{\sin n\pi/2}{n^3} \varphi_n \right| \tag{16}$$

in which φ_n represents the maximum value of the time-function in the n-th mode, and is only a function of the period (or frequency) ratio. The maximum may occur either in the forced phase when the disturbance interacts with the beam or in the free phase which is subsequent to the forced phase. It is noted that Eq.(16) is a rapidly convergent series and it would be adequate by taking the first one or two terms in the series. Also, it is clear that by assigning the maximum value to the time-function in every mode, the result represents an upper bound for the DAF. Analogously, the DAF for a simply-supported plate is:

$$A_p = 1.11 \sum_{m}^{\infty} \sum_{n}^{\infty} \left| (p_{11}/p_{mn})^2 \frac{n^2 + \nu(mr)^2}{mn(1+\nu r^2)} \left(\sin\frac{m\pi}{2} \sin\frac{n\pi}{2}\right) \varphi_{mn} \right| \tag{17}$$

in which φ_{mn} is the maximum value of the time-function in the m-nth mode and is a function of the period ratio only. It is recognized that φ_{mn} is analogous to φ_n in every respect. Thus, in Figure 4, φ_n or φ_{mn} is represented by the same curve which is a function of the appropriate period ratio. It is observed that at large values of period ratio, the curve becomes asymptotic to 2.0. However, the series in Eq.(17) converges slightly slower than that in Eq.(16), therefore six or nine terms in the series are usually required for the desired accuracy for the plate.

Substituting Eq.(15) into Eq.(13), multiplying the resulting equation by Eq.(14) and integrating with respect to ξ, the response of a simply supported beam to an N-shaped wave traveling at a constant velocity v is obtained. In the response equation, there is a velocity which makes both the denominator and numerator vanish and the actual response can only be evaluated by a limiting process. This velocity may be called the coincidence velocity. Further studies indicate [10] that, in the simple case of a single moving load, the absolute maximum modal response of the beam occurs during the forced phase at a velocity (critical velocity) substantially less than the coincidence velocity, but the maximum value is only 12% higher than that computed at the coincidence velocity. Evidently, in the more complicated case of traveling wave, the maximum response would depend also on the exact wave shape and as a result, an extensive numerical computation would be required to find it. On the other hand, it is believed that the results due to the critical and coincidence velocities should not be substantially different, and it is therefore justified to use the coincidence velocity with the great simplification of the problem.

Obviously, the maximum response in the present case occurs when the coincidence velocity corresponds to the fundamental mode of the structural element. The DAF for the simple beam is thus found to be:

$$A'_b = 1.03\ \varphi'_1 \tag{18}$$

where φ'_1 is a function of the fundamental period ratio, R_1, (defined as the ratio of τ to the fundamental period of structure) and is presented in Figure 5. Analogously, the DAF for the simply supported rectangular plate is:

$$A'_p = 1.11\ \varphi'_{11} \tag{19}$$

where φ'_{11} can be also obtained from Figure 5 provided the fundamental period of the plate is used instead of that of the beam for R_1.

We are now in a position to compare the dynamic effects of the N-shaped disturbance on structural elements as it takes the form of either a traveling wave or of a pressure pulse. Due to the rapid convergence of the series in Eqs.(16) and (17), as well as to the fact that Eqs.(18) and (19) are obtained on the basis of the coincidence velocity in a single mode, it is sufficient to compare the

maximum modal responses in the fundamental mode only. The following tabulation gives, side by side, these responses to the traveling wave and the pressure pulse:

Phase \ Disturbance	Traveling Wave	Pressure Pulse
Forced	$\varphi_1' = 1.785$	$\varphi_1 = 2.0$
Free	$\varphi_1' = 1.28$	$\varphi_1 = 2.13$

It is seen that the pressure pulse induces much more severe maximum dynamic effect in structural elements than the traveling wave either in the forced phase or in the free phase.

5. THE EFFECTS OF BOUNDARY RESTRAINTS

In assessing the relative severity of different boundary conditions, it is noted that the real condition of structural elements should be bounded by the limiting cases of simply-supported and clamped-clamped. The simply-supported boundary condition has been studied in the previous section. The clamped-clamped boundary condition in conjunction with an N-shaped pressure pulse will be studied presently.

The basic solutions represented by Eq.(10) is still valid for the clamped-clamped structural elements provided the correct eigenvalue and the correct normalized eigenfunction are used. Since only the symmetrical modes are excited, the origin of coordinate axes can be conveniently taken at the center of span. In the case of clamped-clamped beams, the eigenvalue and the normalized eigenfunction are, respectively:

$$p_n^2 = (m_n/\ell)^4 \, EI/\mu \tag{20}$$

$$z_n(x) = 1/\sqrt{\ell}\left(\cos\frac{m_n x}{\ell}/\cos\frac{m_n}{2} - \cosh\frac{m_n x}{\ell}/\cosh\frac{m_n}{2}\right) \tag{21}$$

where m_n satisfies the frequency equation:

$$\tanh\frac{m_n}{2} + \tan\frac{m_n}{2} = 0 \tag{22}$$

corresponding to the first three symmetrical modes, Eq.(22) gives: $m_2 = 4.73$, $m_4 = 10.996$ and $m_6 = 17.279$. Substituting Eq.(21) into Eq.(9) and performing integration, one gets:

$$C_n = (4/\ell/m_n) \tan \frac{m_n}{2} \tag{23}$$

Using Eqs.(21), (23) and (10) coupled with Eq.(14), the response of the clamped-clamped beam to an N-shaped pressure pulse is found to be:

$$z(x,t) = \frac{4p_o\ell^4}{EI} \sum_{n=\text{even}}^{\infty} \left| \frac{\tan \frac{m_n}{2}}{m_n} \left(\frac{\cos \frac{m_n x}{\ell}}{\cos \frac{m_n}{2}} - \frac{\cosh \frac{m_n x}{\ell}}{\cosh \frac{m_n}{2}} \right) \varphi_n \right| \tag{24}$$

in which φ_n is the same as defined in Eq.(16). The moment along the entire beam can now be evaluated. The maximum moment occurs at the supports having the form of:

$$M_S = 8 p_o \ell^2 \sum_{n=\text{even}}^{\infty} \left| \frac{\tan \frac{m_n}{2}}{m_n^3} \varphi_n \right| \tag{25}$$

whereas the moment at the midspan is:

$$M_C = 8 p_o \ell^2 \sum_{n=\text{even}}^{\infty} \left| \frac{\tan \frac{m_n}{2}}{m_n^3} \left(\frac{1}{\cos \frac{m_n}{2}} + \frac{1}{\cosh \frac{m_n}{2}} \right) \varphi_n \right| \tag{26}$$

The DAF can now be evaluated by using the static moment at the support ($p_o \ell^2/12$) and that at the center ($p_o \ell^2/24$). It is found that the DAF at the center is, in general, higher than at the support, but is always much less than twice as much. Consequently, the maximum dynamic moment always occurs at the support. However, in comparing with the maximum dynamic moment in a simply-supported beam, it is still much less. Therefore, unless the boundary condition is clearly clamped-clamped, it would be more realistic to assume the simply-supported condition.

A similar treatment for square plate is also made. It is found that although the dynamic moment at the midpoint of the clamped edge is bigger than at the center, it is far smaller than what would be induced at the center of a simply-supported plate. The same conclusion may also be drawn for rectangular plates.

6. STRUCTURAL RESPONSE TO VARIOUS IDEALIZED BOOM SIGNATURES [12]

The fact that the sonic boom signature may vary widely as seen in Figure 1 makes it desirable to study the response of the structural elements to each of these realistic boom signatures. To simplify analysis, these boom signatures are idealized as shown in Figure 6. As pressure pulses, they may be described mathematically as follows:

(a) Sine pulse

$$P(t) = \sin 2\pi\tilde{t}\,[1 - H(\tilde{t}-1)] \tag{27a}$$

(b) Half-Cosine pulse

$$P(t) = \cos \pi\tilde{t}\,[1 - H(\tilde{t}-1)] \tag{27b}$$

(c) Triangular pulse

$$P(t) = \tilde{t}/\tilde{s} - [(\tilde{t}-\tilde{s})/\tilde{s}(1-2\tilde{s})]\,H(\tilde{t}-\tilde{s}) + [(\tilde{t}-1+\tilde{s})/\tilde{s}(1-2\tilde{s})]H(\tilde{t}-1+\tilde{s}) - [(\tilde{t}-1)/\tilde{s}]H(\tilde{t}-1) \tag{27c}$$

(d) N-Shaped pulse with Spikes

$$P(t) = (1+\alpha) - (2+\alpha/\beta)\tilde{t} - \alpha(1-\tilde{t}/\beta)H(\tilde{t}-\beta) + [(1+\alpha) - (2-\alpha/\beta)(1-\tilde{t})]H(\tilde{t}-1) - (\alpha/\beta)(1+\beta-\tilde{t})\,H(\tilde{t}-1+\beta) \tag{27d}$$

where $\tilde{t}=t/\tau$, $\tilde{s}=t_1/\tau$ and t_1 is the rise time for the triangular pulse. α and β are dimensionless coefficients defining the shape of a spike. It may be verified that when $\tilde{s}$ vanishes in Eq.(27c) and α or β vanish in Eq.(27d), the corresponding forcing functions all reduce to the N-shaped pulse.

The dynamic response of a continuous system such as a beam or a plate consists of an infinite sum of the products of the mode shape function and the time function of all the modes. If one is interested in the upper bound of the response, the maximum values can be assigned to both the mode shape function and the time function. The time function, however, must satisfy an equation identical to Eq.(4), or:

$$\ddot{T}_n + p_n^2 T_n = \frac{1}{\mu} P(t) \tag{28}$$

It is noted that Eq.(28) governs the motion of a single oscillator of frequency p_n which may be defined as $\sqrt{k/\mu}$, and k being the spring constant. The maximum response of the oscillator to the disturbance p(t) having the maximum amplitude of unity is thus:

$$|T_n|_{max} = \left|\frac{1}{\mu p_n}\int_o^t P(\xi) \sin p_n(\xi - t)d\xi\right|_{max} = \varphi_n/\mu p_n^2 \qquad (29)$$

in which φ_n has been previously defined in Eq.(16). Defining the dynamic amplification function (hereafter daf) as the ratio of the maximum response of the single oscillator to the static response which is simply 1/k, one finds:

$$\text{daf} = \varphi_n \qquad (30)$$

It is noted that the daf or φ_n is the component in the series for the DAF given by Eqs. (16) and (17). It is clearly advantageous to attempt to obtain first the daf before constructing the DAF for all the idealized boom signatures. Due to the rapid convergence of the series for the DAF, only a few terms of daf would be necessary for an adequate accuracy. Further, should it become important to consider the effect of damping, it can be easily accomplished through the use of a simple analog computer.

Neglecting damping for the time-being, the forcing functions in Eq.(27) can be substituted in Eq.(29) and the daf or φ_n determined in the usual manner for any given period ratio. Thus Figure 7 shows the daf as a function of the period ratio R for a sine pulse. Similarly, Figure 8 gives the daf for a half-cosine pulse. It must be pointed out that they represent the envelopes of maximum daf at a given R, which may occur either during the forced phase or in the subsequent free phase. An inspection reveals that the sine pulse induces a maximum daf of more than 3.25, but at large values of R, the daf tends to be asymptotic to unity. On the other hand, the half-cosine pulse induces a maximum daf of about 2.70, and the daf is asymptotic to 2.0 at large values of R. Comparing it with the daf for an N-shaped pulse (Figure 4), the latter induces a maximum of 2.23 and is also asymptotic to 2.0 at large values of R. The smaller peak value in the case of the N-shaped pulse seems to be due to the sharper decay of the pressure jump resulting in a smaller positive impulse (positive area enclosed in the pulse diagram).

Obviously the positive impulse is not the sole factor affecting the maximum value of daf. Figure 9 shows a comparison of the daf envelopes for several symmetrical triangular pulses having different rise times. Since every pulse has the identical positive impulse, the diagrams serve to reveal, in addition to their intrinsic values, the effect of the rise time ratio, $\tilde{s}$. At R below 0.8, it is seen that the daf is insensitive to $\tilde{s}$, one may conclude that it is dependent solely on the positive impulse for relatively low values of R. Also, the peak daf increases with $\tilde{s}$, while the value of R at which the peak

occurs shifts from below to above unity. But even at $\tilde{s} = 0.25$, the peak daf is still substantially below that corresponding to the sine pulse. At large values of R, the peak daf seems to be again asymptotic to 2.0.

Figure 10 gives the daf envelopes for an N-shaped pulse with spikes. The parameter α is taken to be unity, meaning that the spike is of equal magnitude as the peak pressure of the basic N-shaped pulse. The parameter β is given three different values namely, .1, .05 and .01. For the smallest β, the disturbance is almost like a perfect N-shaped pulse, and the diagram should be comparable to what is given in Figure 4. However, since the daf is obtained on the basis of peak pressure, which is $(1+\alpha)p_o$ or $2p_o$ in the present case, the magnitude of daf is about half of that for a perfect N-shaped pulse.

As expected, Figure 10 shows that the daf increases with β which is a measure of the positive impulse of the disturbance. In addition, it is seen that the daf increases also with R. Further investigations, however, reveal that the daf is, in a practical sense, bounded and remains below 2.5 for R as large as 50. Results for $\alpha = 0.5$ are found to be consistently lower, hence not presented here.

Once the daf or φ_n as a function of R is obtained for a given disturbance, the DAF can be easily constructed. For a simple beam, for instance, Eq.(16) may be written in the following form:

$$A_b = 1.03 \left(\varphi_1 + \bar{\varphi} \sum_{n=3,5}^{\infty} \frac{1}{n^3} \right) = 1.03(\varphi_1 + .05\bar{\varphi}) \qquad (31)$$

where $\bar{\varphi}$ is the asymptotic value of φ_n at large values of R, and φ_1 is the daf corresponding to the fundamental mode. Since the period ratio corresponding to the next higher mode than the fundamental is nine times as large, it is justifiable to factor out $\bar{\varphi}$ in Eq.(31). Similarly, for a square plate ($\nu = 0.3$), Eq.(17) may be approximated as:

$$A_p = 1.11 \, (\varphi_{11} + 0.19\bar{\varphi}) \qquad (32)$$

where $\bar{\varphi}$ represents the asymptotic value of φ_{mn} at large R and φ_{11} the daf for the fundamental mode. For an N-shaped as well as a half-cosine pulse, $\bar{\varphi}$ takes an asymptotic value of 2.0; whereas for a sine pulse $\bar{\varphi}$ can be taken as one. Since φ_1 and φ_{11} depend only on the fundamental period of the structural element, the DAF become simply a function of the fundamental period ratio, R_1, only.

As it has previously been noted that the DAF so obtained is the upper bound of the true DAF, because it is obtained on the assumption that all the daf simultaneously reach their respective maxima. In an effort to assess the accuracy of the upper bound approach, the DAF for a simple beam subjected to an N-shaped pulse is obtained through a direct numerical evaluation of the response series at

small time intervals and with an automatic comparing and elimination process. The DAF so obtained is presented in Figure 11 alongside with that obtained by Eq.(31). It is seen that the results by either method are comparable. Since the upper bound method is much simpler and somewhat more conservative, its use is considered justified.

In concluding the study of structural response to various boom signatures, it is seen that, in general, the DAF is dependent on both the period ratio and the exact shape of the signature. For a given shape of boom signature, the DAF can be reduced to depend only on the fundamental period ratio for the structural element.

7. EFFECTS OF DAMPING [12]

It is only realistic to take into account the effects of damping although the complication introduced may be considerable. The time function now must satisfy the following equation:

$$\ddot{T}_n + 2\zeta p_n \dot{T}_n + p_n^2 T_n = \frac{1}{\mu} P(t) \qquad (33)$$

If the forcing function is an N-shaped pulse, the damped daf varies with the period ratio as shown in Figure 12. While the solid lines represent the results of analytical solution, the small circles represent the analog computer results. The confirmation of the analytical results by the use of an analog computer is rather good. Similarly, the damped daf for a half-cosine pulse and for a sine pulse are shown in Figures 13 and 14, respectively. It should be noted that in these figures, dotted curves pertaining to damping factors ζ equal to .025 and .05 are obtained exclusively by the analog computer.

An inspection of Figure 12 reveals that the effect of damping depends on the period ratio, and it becomes particularly effective near the integer values of the period ratio. The reason for all this can be seen from Figure 15 in which the critical time-ratio corresponding to the absolute maximum response is plotted against the period ratio. It is noted that near the integer value of the period ratio, the maximum occurs either in the free phase ($t_c/\tau > 1$) or near the end in the forced phase. In both cases, the damping is expected to be substantial since damping effect is proportional to the number of cycles of oscillation.

It is clear then damping should be more effective for stiff structural elements or for large period ratios. This is borne out in Figure 16 by plotting the critical time-ratio against the period ratio for a small amount of damping (ζ=.025). The critical time-ratio is seen to have shifted from around unity to a

fraction as long as the period ratio is slightly above 2.0. The same is found to be true for the half-cosine pulse. For the N-shaped pulse with spikes, the sharp increases of the daf around integer values of period ratio (Figure 10) are believed to be affected by damping and are likely to be replaced by a gradually ascending curve asymptotic to 2.0.

Inasmuch as there always exists a certain amount of damping, one may conclude that the maximum is likely to occur near the zero time at large period ratios. Under this circumstance, as far as the structural element is concerned, the loading essentially behaves like a step loading. Consequently, the daf should never exceed 2.0 at large period ratios.

8. A SIMPLIFIED APPROACH TO EVALUATING EFFECTS OF SONIC BOOMS [12]

Previous sections have shown that the DAF depends in general on the exact shape of boom signature and on the period ratio. Due to the rapid convergence of the series, and to the asymptotic behavior of the daf at large values of the period ratio, the DAF can be made dependent only on the fundamental period ratio provided the shape of boom signature is prescribed. Unfortunately, due to a variety of circumstances, the exact shape of boom signature that interacts with the structural element may always be somewhat uncertain. Hence, from a practical point of view, it seems more important to devise an approach by which an engineering assessment of the sonic boom effects can be made simply, quickly and with the minimum number of parameters.

At the expense of accuracy which may be somewhat sacrificed for practical purposes, two simplified methods may be proposed. In both methods, the fundamental period ratio (R_1) must be known. The additional parameter in the first method is simply the peak pressure (p_o); and in the second, the positive impulse (I_o). The two methods are closely related and require no knowledge of the exact shape of the boom signature as will be explained below:

(A) Simplified DAF Envelopes

To circumvent the requirement of knowing the exact shape of boom signature, it is proposed to construct a realistic governing envelope using all the daf envelopes so far obtained for the various boom signatures. As an intermediate step, a set of damped daf envelopes are constructed and shown in Figure 17. For all practical purposes, the sine pulse governs the envelope within a narrow range of the period ratio ($0.8 \leq R \leq 1.90$), and the half-cosine pulse governs it outside of this range. Noting that the asymptotic value of daf for the sine pulse is unity and that for the half-cosine pulse is two, the DAF for the beam, or

Eq.(31) may be written as:

$$\begin{aligned} A_b &= 1.03\,(\varphi_1 + 0.05), \qquad 0.8 \le R_1 \le 1.90 \\ A_b &= 1.03\,(\varphi_1 + 0.1)\ , \qquad 0 \le R_1 < 0.8 \text{ and } R_1 > 1.90 \end{aligned} \tag{34}$$

Similarly, the DAF for the square plate, or Eq.(32) becomes:

$$\begin{aligned} A_p &= 1.11\,(\varphi_{11} + 0.19), \qquad 0.8 \le R_1 \le 1.90 \\ A_p &= 1.11\,(\varphi_{11} + 0.38), \qquad 0 \le R_1 < 0.8, \text{ and } R_1 > 1.90 \end{aligned} \tag{35}$$

In addition, assuming the existence of some damping, then at a sufficiently large value of R_1, the disturbance can be viewed as a step loading. Therefore, it is proposed that:

$$A_b = A_p = 2.0, \quad \text{at} \quad R_1 > 2.25 \tag{36}$$

Using Eqs.(34) to (36) and Figure 17, an envelope for A_b and A_p can be constructed within the specified ranges of R_1. To further simplify the envelopes, straight lines are used as shown in Figure 18. It should be clear that in constructing the envelopes, the effect of damping is ignored for relatively flexible structures (small R_1) and is implicit for relatively stiff structures (large R_1).

The static moment to be used in a simple beam is $p_o \ell^2/8$ and that in a simple square plate, $0.0479\, p_o a^2$. Knowing p_o, the dynamic moments can now be evaluated.

(B) Simplified Envelopes for Dynamic Moment Coefficients

If the positive impulse I_o instead of the peak pressure is known, another method may be devised since the envelope of DAF is available. Noting that the quantity $p_o \tau / I_o$ is a numerical constant (π) for both since and half-cosine pulses, the following expression may be written:

$$\text{DAF} = K I_o / p_o \tau \tag{37}$$

where K depends on R_1 and may be obtained by multiplying the DAF by π. However, a study of field measurements [8] of sonic boom disturbance indicates an average value of $p_o \tau / I_o$ about 4 (instead of π) for a sine pulse; 4.35 (instead of 4) for an N-shaped pulse and 5 (instead of slightly over 4) for an N-shaped pulse with spikes. Obviously, I_o is always less in reality than in the idealized wave shapes, and it becomes accentuated in the case with spikes where the

pressure decay is very steep. Therefore, in constructing Figure 19, a value of 4 is used for $p_o\tau/I_o$ at $R_1 \leq 1.25$ and 5 at $R_1 > 2.25$. Straight lines are used in connecting the diagrams in the intermediate region.

Using the definition of the DAF, the dynamic moment for the beam and plate can be obtained respectively as follows:

$$M_{db} = K_b I_o \ell^2/8\tau$$
$$M_{dp} = 0.0479 K_p I_o a^2/\tau \qquad (38)$$

K_b and K_p may be called the dynamic moment coefficient for beam and plate respectively.

It is believed that comparable results can be obtained by either of the two simplified methods. While the first is more accurate, the second should be more conservative for most wave shapes except for those with sharp spikes for which the results may be somewhat lower for very stiff structural elements.

9. CONCLUDING REMARKS

Allowing certain variabilities of shape of sonic boom signatures as reflected in field measurements, an upper-bound of the dynamic effects on structural elements may be estimated by the simplified method reported herein. Aside from the usual assumptions regarding the structural element, it is understood that it is always in contact with the supports. Furthermore, the sonic boom effects are considered super-imposable to other effects, either static or dynamic, due to other causes.

Considerably higher dynamic effects can be expected in the unusual case where the structural element is loosely bound to supports and can therefore rattle in the wake of sonic boom disturbances. Depending on the relative stiffness of the structural element and its support and other factors, the dynamic shear may increase much more rapidly than the dynamic moment. As a result, the tensile stress induced by shear at the supports may become the dominant cause for damage in structural elements made of brittle construction material. This is illustrated in the Appendix by a rattling beam subjected to an N-shaped pulse.

BIBLIOGRAPHY

[1] Hubbard, H.H.
Nature of the Sonic-Boom Problem
J. Acoust. Soc. Am. 39, No.5, pt.2, 1966. Sonic Boom Symposium, pp s1-s9.

[2] Whitham, G.S.
The Flow Pattern of a Supersonic Projectile
Commu. Pure Appl. Math. 5, No.3, 1952, pp 301-348.

[3] Carlson, H.W., Mack, R.J. and Morris, O.A.
Sonic-Boom Pressure-Field Estimation Techniques
J. Acoust. Soc. Am. 39, No.5, pt. 2, 1966. Sonic Boom Symposium, pp s10-s18.

[4] Lansing, D.L. and Maglieri, D.J.
Comparison of Measured and Calculated Sonic-Boom Ground Patterns due to Several Different Aircraft Maneuvers
NASA TN-D-2730, 1965.

[5] Maglieri, D.J.
Some Effects of Airplane Operations and the Atmosphere on Sonic Boom Signatures
J. Acoust. Soc. Am. 39, No.5, pt. 2, 1966. Sonic Boom Symposium, pp s36-s42.

[6] Garrick, I.E. and Maglieri, D.J.
Variability of Sonic Boom Pressure Signatures Associated with Atmospheric Conditions
Paper presented at Int. Assoc. Meteor. Atm. Phys., Switzerland, 1967.

[7] Hubbard, H.H., Maglieri, D.J., Huckel, V. and Hilton, D.A.
Ground Measurements of Sonic-Boom Pressures for the Altitude Range of 10,000 to 75,000 Feet
NASA TR R-198, 1964.

[8] Hilton, D.A., Huckel, V., Steiner, R. and Maglieri, D.J.
Sonic Boom Exposure During FAA Community-Response Studies Over a 6-Month Period in the Oklahoma City Area.
NASA TN D-2539, 1964.

[9] National Sonic Boom Evaluation Office
Sonic Boom Experiments at Edwards Air Force Base
Interim Report, 1967.

[10] Cheng, D.H. and Benveniste, J.E.
Transient Response of Structural Elements to Traveling Pressure Waves of Arbitrary Shape
Presented at the 5th U.S. Nat. Cong. App. Mech. 1966
Int. J. Mech. Sci., 8, 1966, pp 607-618.

[11] Crocker, M.J.
Multimode Response of Panels to Normal and to Traveling Sonic Booms
J. Acoust. Soc. Am., 42, No.5, 1967.

[12] Cheng, D.H. and Benveniste, J.E.
Sonic Boom Effects on Structures - A Simplified Approach
Trans. N.Y. Acad. Sci. Ser. II, V.30, No.3, pp 457-478, Jan.1968.

[13] Benveniste, J.E. and Cheng, D.H.
Sonic Boom Effects on Beams Loosely Bound to Their Supports
Presented at the AIAA 5th Aerospace Sciences Meeting, 1967
J. Aircraft, 4, No.6, 1967.

[14] Wiggins, J.H. Jr., and Kennedy, B.
Theoretical Study of Structural Response to Near-Field and Far-Field Sonic Booms
Final Report, Contr. No. AF 49 (638) - 1777, Datacraft Inc. 1966.

[15] Lowery, R.L. and Andrews, D.K.
Acoustical and Vibrational Studies Relating to an Occurrence of Sonic Boom Induced Damage to a Window Glass in a Store Front
NASA CR-66170, 1966.

APPENDIX

RESPONSE OF STRUCTURAL ELEMENTS LOOSELY BOUND TO SUPPORTS SUBJECTED TO N-SHAPED PULSE

In the text of this report, the structural elements are assumed to be always in contact with non-yielding supports. However, in houses of sub-standard construction or in disrepair, structural elements such as window panes are often found to be not in immediate contact with the supporting frame. A disturbance in the form of a pressure pulse will induce rattling of the element within a gap, possibly resulting in dynamic effects much more severe than those predicted by the previous treatment.

It would seem desirable to treat a uniform, rectangular or square plate subjected to an N-shaped pressure pulse; the plate would be induced to rattle in a gap between two sets of springs. The assumption of spring supports seems not only realistic, but also it circumvents a serious difficulty which arises when the classical plate theory is used in the case of rigid supports. However, one major difficulty still remains for the plate, that is, after its first contact with the spring, new contacts or loss of contact with the spring will not occur simultaneously along the entire perimeter, thus the problem becomes highly indeterminate and untractable.

In an effort to gain some basic understanding of this realistic problem, an analogous problem is studied, namely, a beam which is induced to rattle between two sets of springs by an N-shaped pressure pulse. It is believed that the results obtained for the beam should be more severe than for the plate. The detailed mathematical derivations can be found in Reference 13.

The beam is assumed to be initially at rest (Figure 20). Neglecting damping, the solution can be expressed in two eigenfunction series:

$$Z(x,t) = \sum_{n=1}^{\infty} Z_n^f(x)\ T_n^f(t) \qquad \text{if } q \text{ is even}$$

$$Z(x,t) = \pm a' + \sum_{n=1}^{\infty} Z_n^s(x)\ T_n^s(t) \qquad \text{if } q \text{ is odd} \tag{A1}$$

where q is a phase indicator whose initial value is 0 and which increases by one every time the beam either comes into contact or loses contact with the spring supports. The superscripts f and s denote free-free and spring-supported, respectively. The eigenfunctions $Z_n(x)$, are obtained by satisfying the following equation:

$$L\,Z + p_n^2\,Z = 0 \tag{A2}$$

and the accompanying boundary conditions:

$$Z''_{(\ell/2)} = Z''_{(-\ell/2)} = 0$$

$$EIZ'''_{(\ell/2)} = SZ_{(\ell/2)}, \quad EIZ'''_{(-\ell/2)} = -SZ_{(-\ell/2)} \tag{A3}$$

The time function, T_n on the other hand, must satisfy an ordinary differential equation identical to Eq.(28) and the appropriate initial conditions which are determined inductively. Let $t = t_q$ be the beginning of phase q, then at $t_o = 0$, $T_n(t_o) = \dot{T}_n(t_o) = 0$. Since the response in phase $q-1$ is already determined, t_q is simply the smallest root exceeding t_{q-1} of $|Z(\pm \ell/2, t)| = a'$. For $t = t_q$, the displacement and velocity of every point on the beam must be continuous, i.e.

$$\sum_{n=1}^{\infty} Z_n^f(x)\, T_n^f(t_q) = \sum_{n=1}^{\infty} Z_n^s(x)\, T_n^s(t_q) \pm a'$$

$$\sum_{n=1}^{\infty} Z_n^f(x)\, \dot{T}_n^f(t_q) = \sum_{n=1}^{\infty} Z_n^s(x)\, T_n^s(t_q) \tag{A4}$$

using the orthogonality properties of the eigenfunction, the initial values $T_n(t_q)$ and $\dot{T}_n(t_q)$ can be obtained via the above equation in terms of the time factors determined in the previous phase. Then by Duhamel's integral, we get:

$$T_n(t) = \frac{\dot{T}_n(t_q)}{p_n} \sin p_n(t-t_q) + T_n(t_q) \cos p_n(t-t_q) + \frac{C_n}{\mu p_n} \int_{t_q}^{t} \sin p_n(t-\xi)\, P(\xi)\, d\xi \tag{A5}$$

where C_n is the Fourier coefficient for the eigenfunction, and $P(\xi)$ is given by Eq.(14). Performing integration, we get finally:

$$T_n(t) = \frac{\dot{T}_n(t_q)}{p_n} \sin p_n(t-t_q) + T_n(t_q) \cos p_n(t-t_q) + \frac{C_n p_o}{\mu} H(\tau - t_q) \left\{ \left[\frac{\cos p_n(t-\tau)}{p_n^2} + \frac{2 \sin p_n(t-\tau)}{p_n^3 \tau} \right] [H(\tau-t) - 1] - \frac{\cos p_n(t-t_q)}{p_n^2}(1 - 2t_q/\tau) + \frac{2 \sin p_n(t-t_q)}{p_n^3 \tau} + \frac{1}{p_n^2}(1 - 2t/\tau) H(\tau - t) \right\} \tag{A6}$$

Equation (A6) together with the appropriate eigenfunction can now be used in Eq.(A1) to compute the end deflection and shear, center deflection and center moment. The computations for the DAF are carried out by using 5 terms in each series at small time intervals until the time $\tau + 3T_1'$, where T_1' is the fundamental period of the free-free beam.

The pertinent parameters in determining the DAF are listed below:

(a) ratio of stiffness of beam and that of spring support, $K' = EI/S\ell^3$;

(b) ratio of boom duration and the fundamental period of free-free beam, $R_1' = \tau/T_1'$;

(c) ratio of half-gap to beam span, $A = a'/\ell$ and

(d) ratio of center deflection under uniform peak pressure to span length, $R_d' = 5\,p_o\,\ell^3/384\,EI = 5\,R_d/384$.

A qualitative understanding is gained by computing the DAF for moment and shear while making some discrete variation for some of the parameters and continuous variation for R_1'. The results are shown in Figures 21 and 22. R_d is chosen to be 0.2133 which corresponds to 1/360 for the ratio of center deflection to span length; A is chosen to be 0.00125 which corresponds to a gap equal to the thickness of a realistic window pane and K is given two values 0.01 and 0.001 which correspond to ratios of center deflection to support deflection of 2.6 and 26 respectively.

It can be seen that for the cases considered, the DAF for moment exceeds 4 whereas that for shear exceeds 6.65, thus both are much more severe than the ordinary simple beam constrained not to rattle. It is noteworthy that shear increases much more readily than moment due to an increase in spring stiffness. This trend is found to continue when a value of K equal to 0.0001 is considered. The case in which K is smaller than 0.0001 is not considered due to inaccuracy introduced by the extremely rapid change of phases. There is also the possibility that the Bernourilli-Euler beam theory itself may not be valid for such stiff supports.

Further computations indicate that for given R_1', K and R_d the gap ratio has only a minor effect on the DAF. The same is true of R_d for given R_1', K and A.

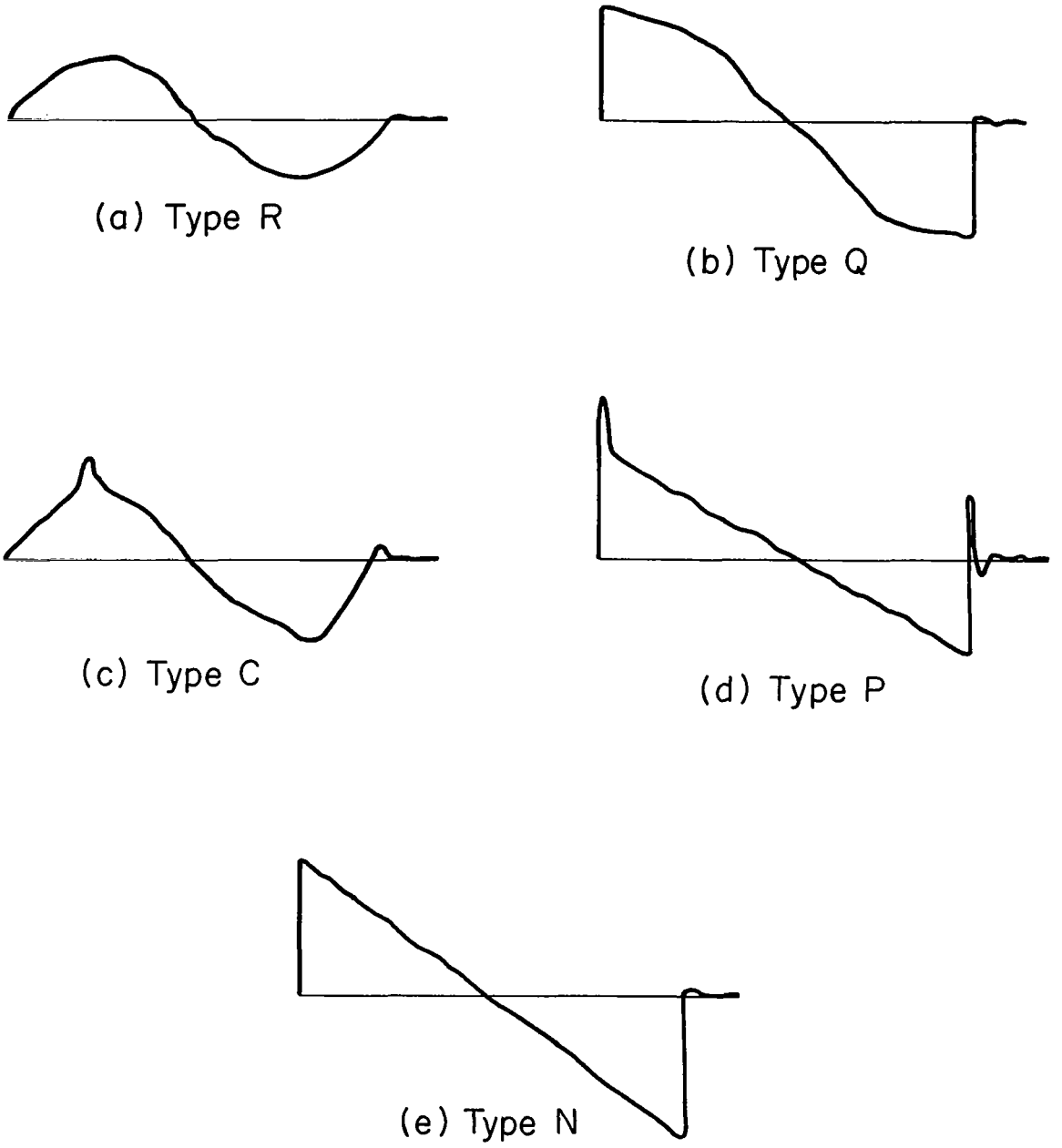

FIGURE 1. Typical sonic boom signatures.

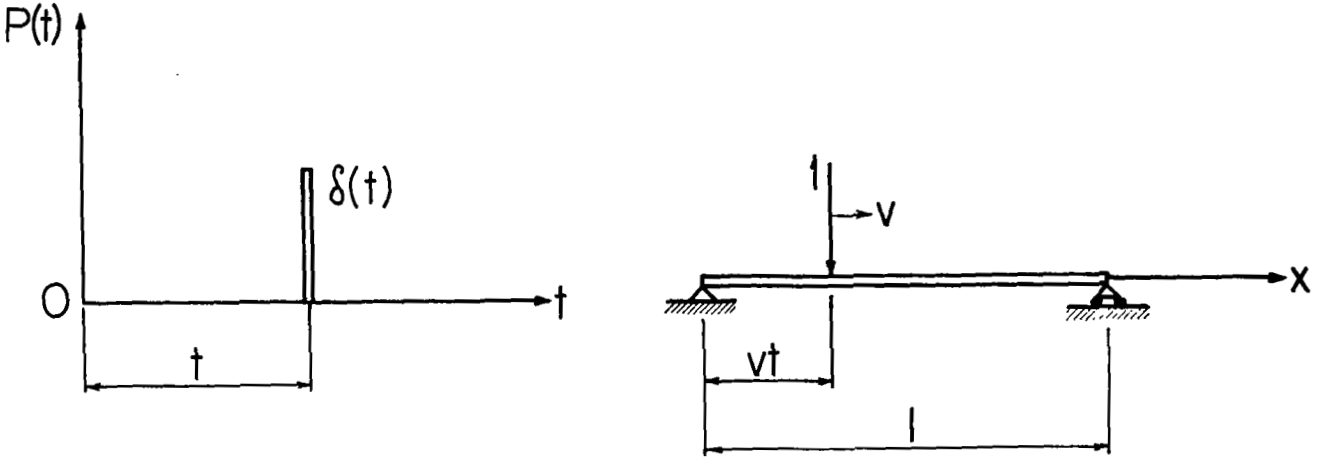

a) Unit impulse.

b) Unit force moving at constant velocity.

FIGURE 2. UNIT DISTURBANCES

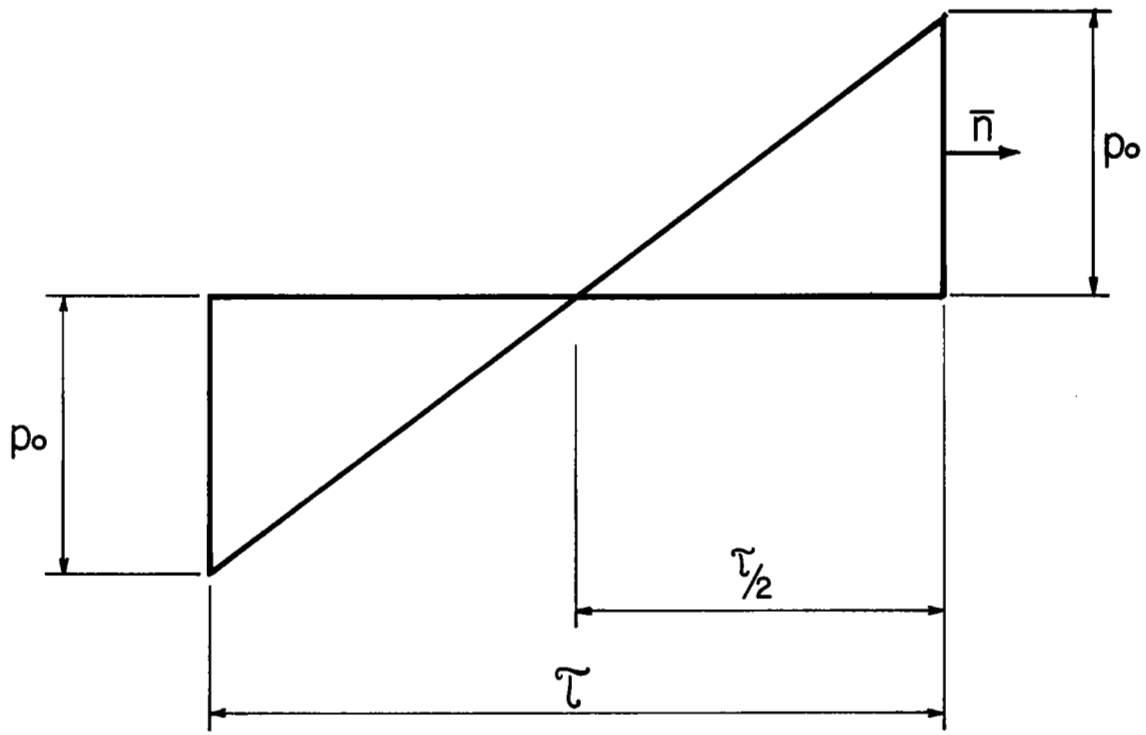

FIGURE 3. N-shaped disturbance (pulse or traveling wave).

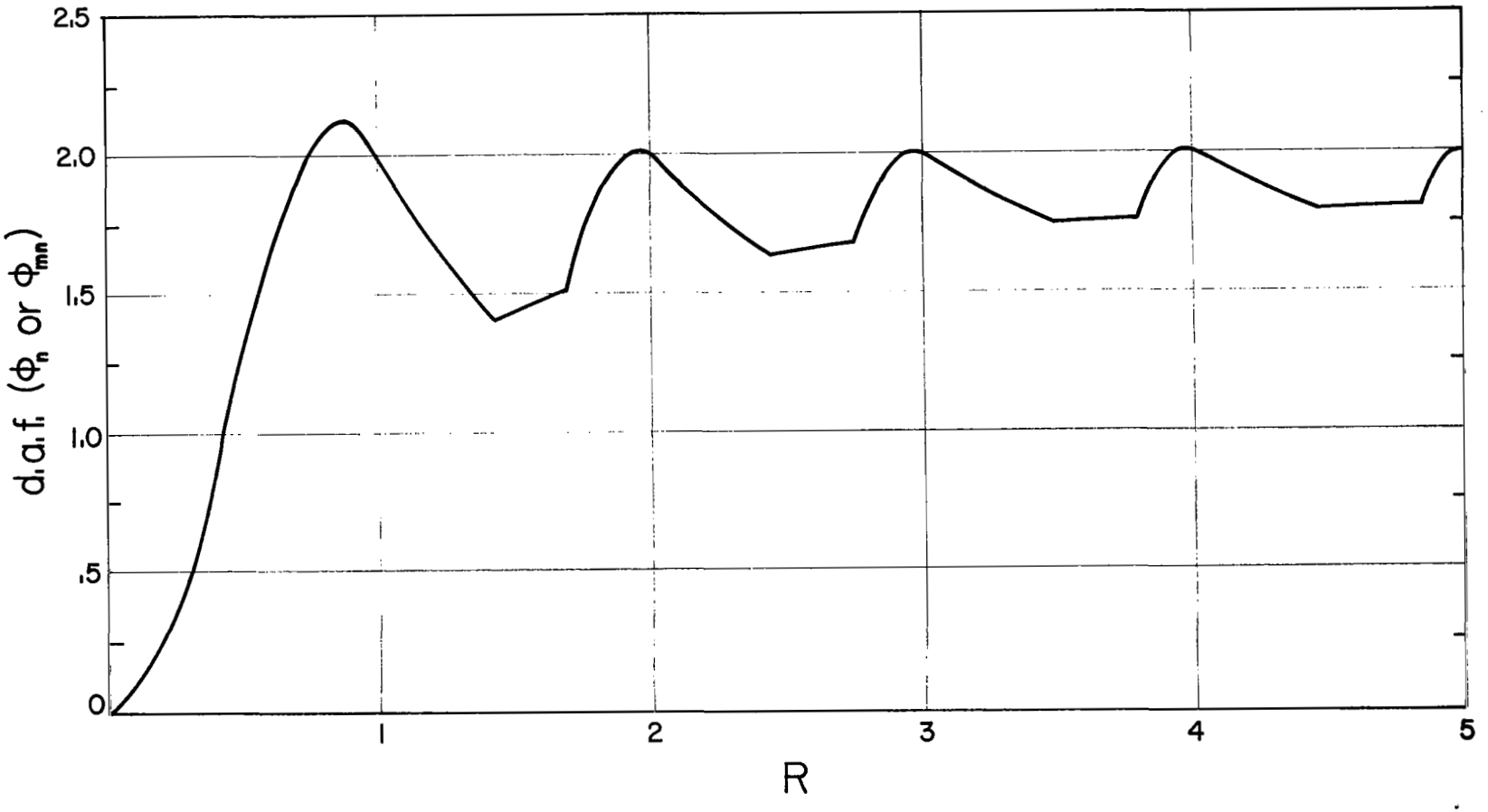

FIGURE 4. Maximum modal response to N-shaped pulse.

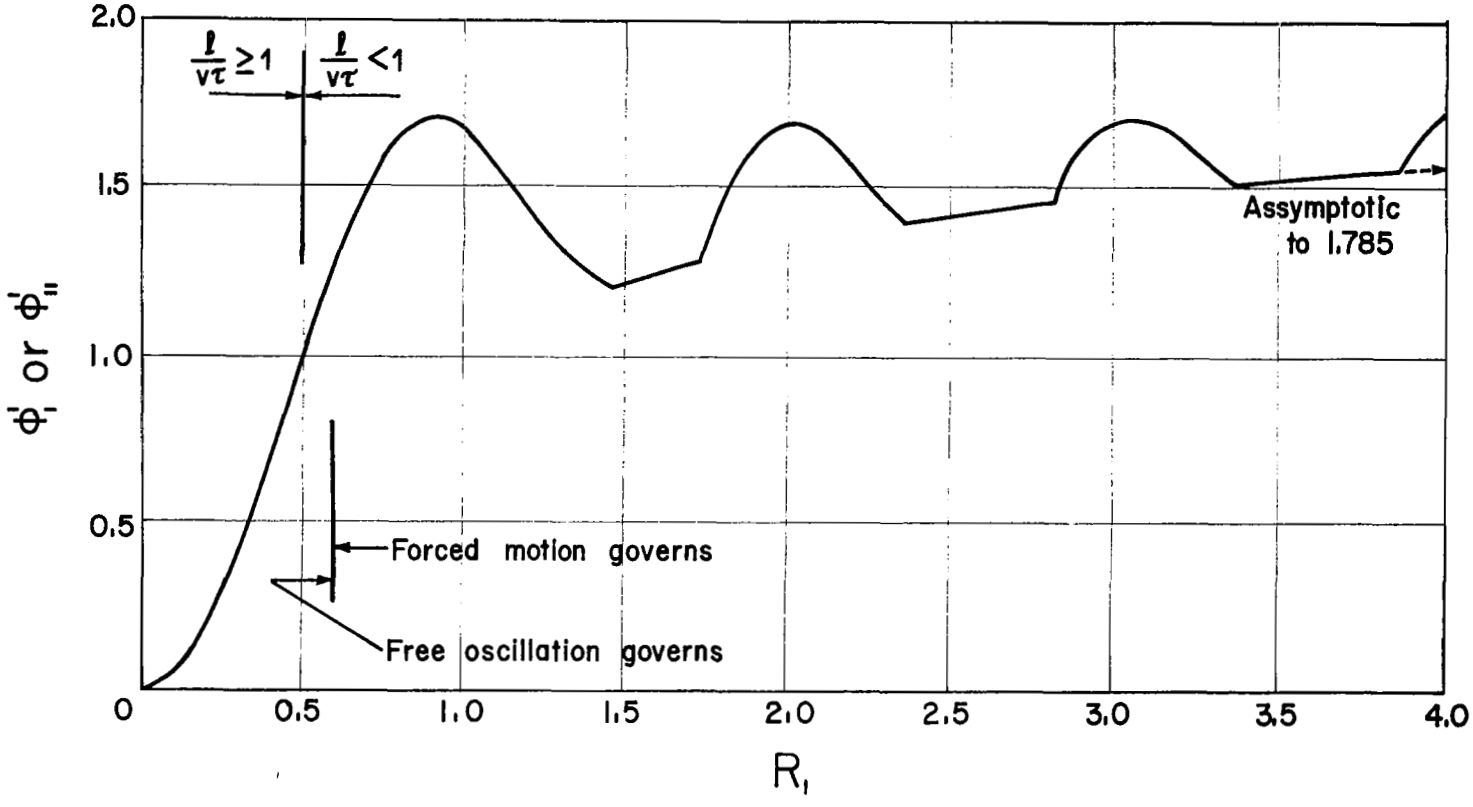

FIGURE 5. Maximum modal response to N-shaped traveling wave.

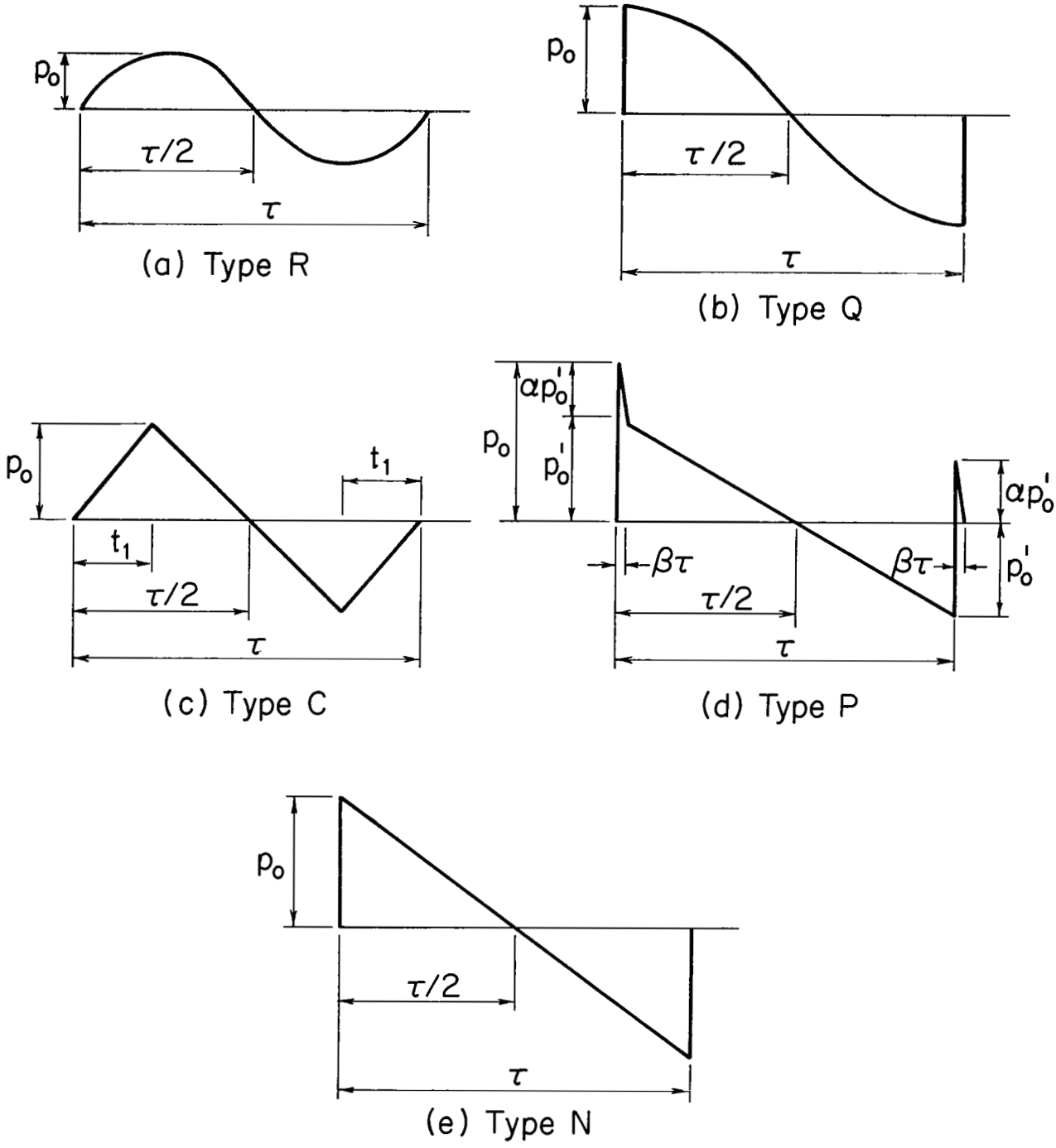

FIGURE 6. Idealized sonic boom signatures.

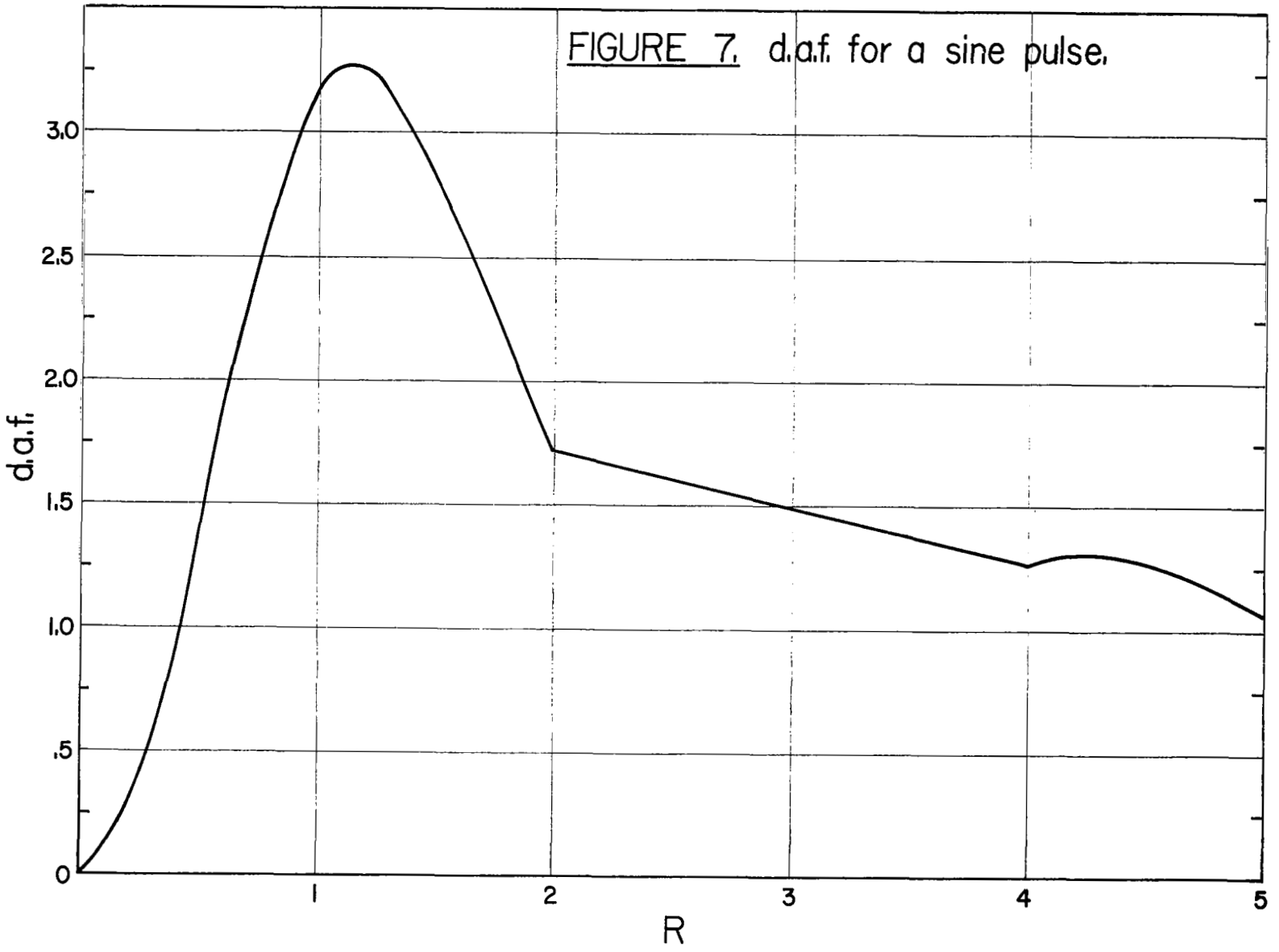

FIGURE 7. d.a.f. for a sine pulse.

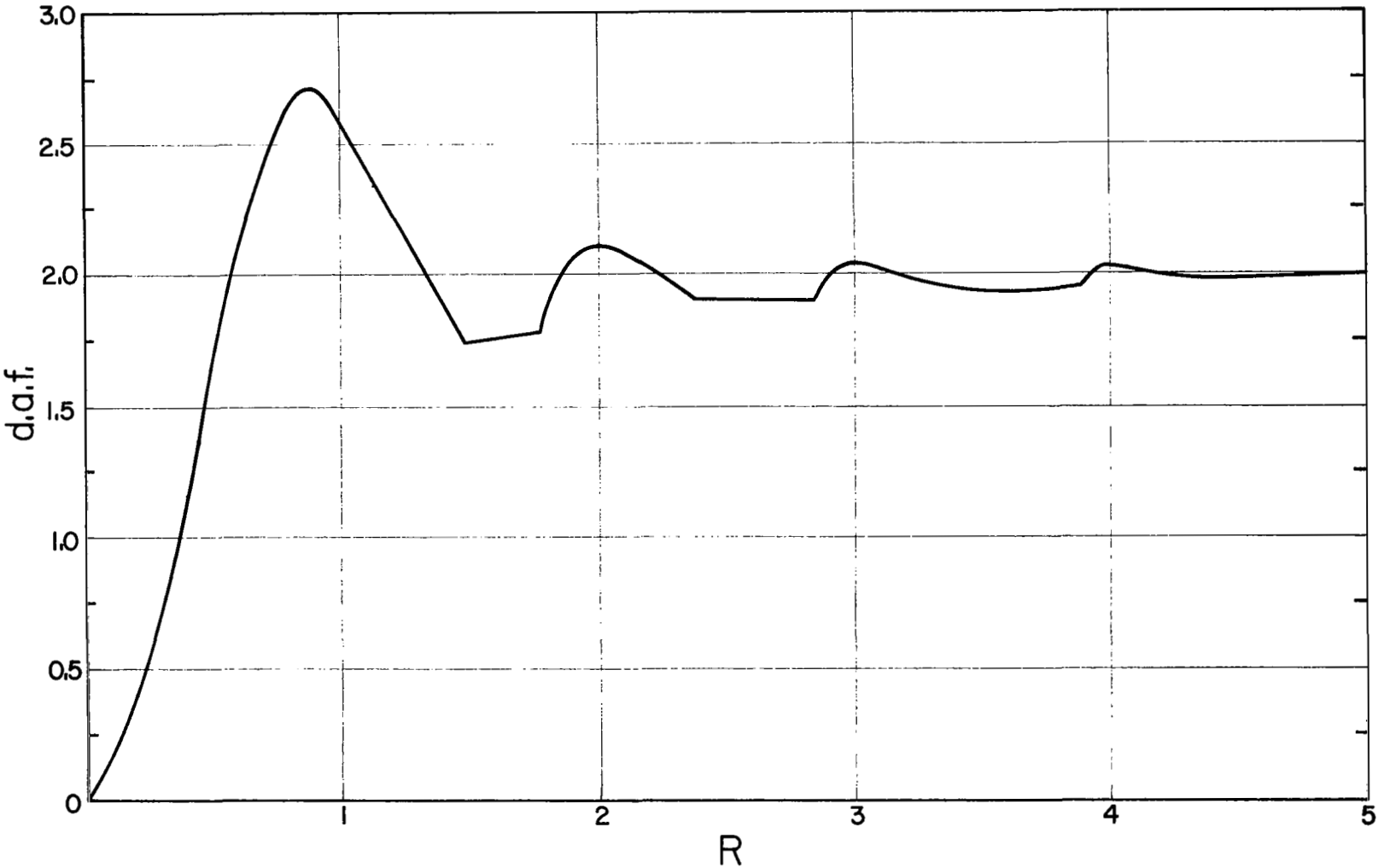

FIGURE 8. d.a.f. for a half-cosine pulse.

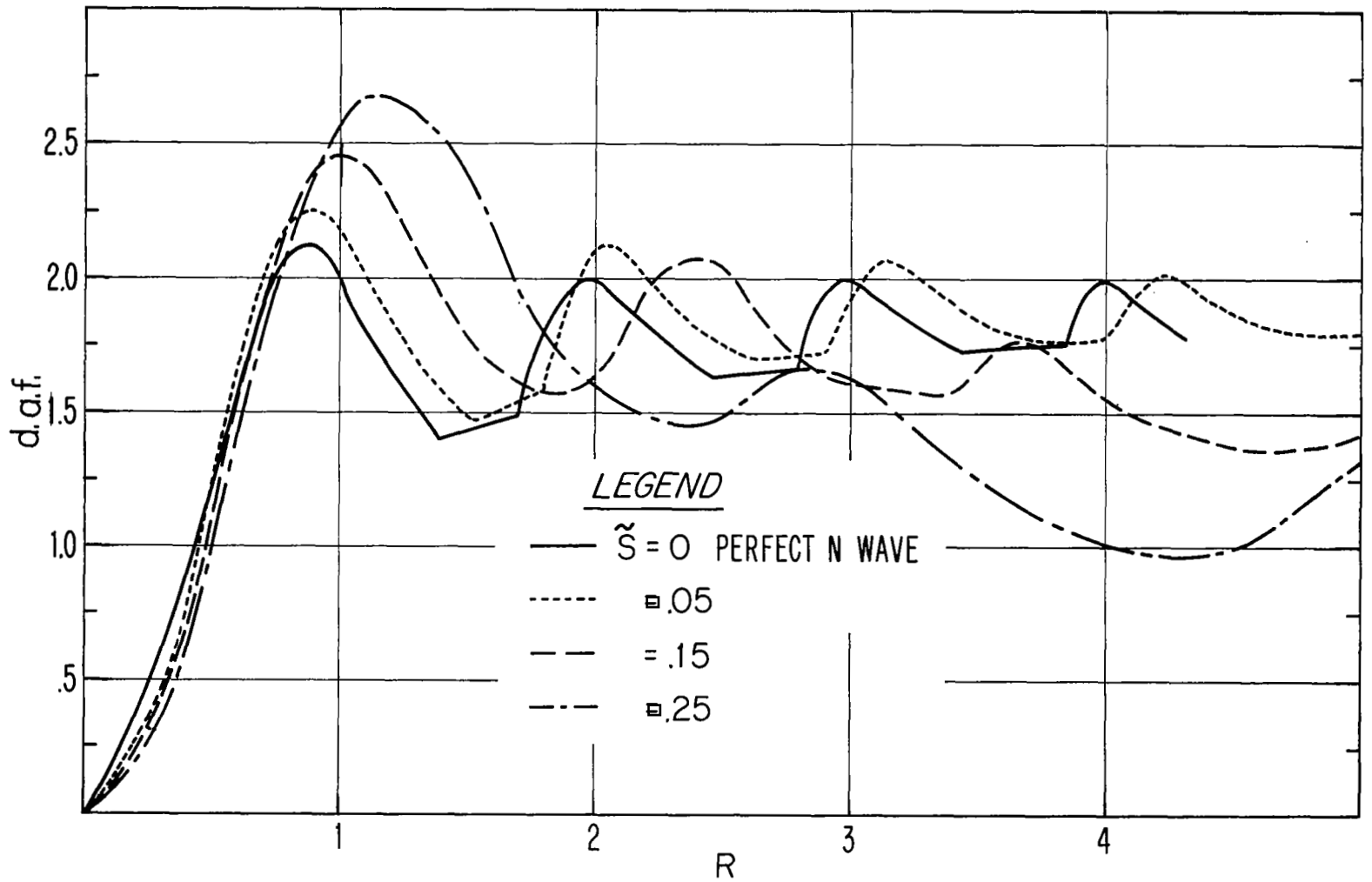

FIGURE 9. d.a.f. for triangular pulses.

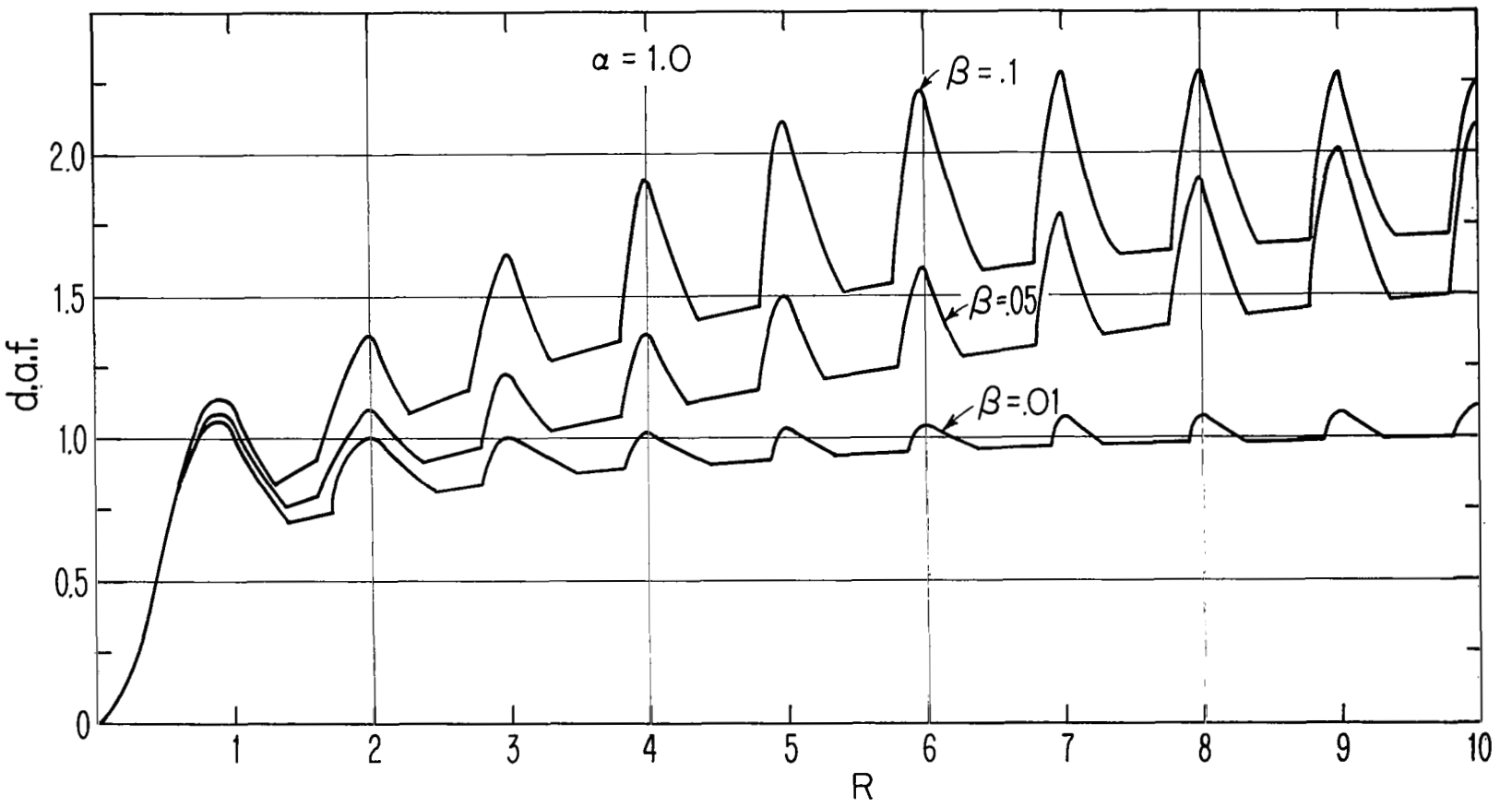

FIGURE 10. d.a.f. for an N-shaped pulse with spikes.

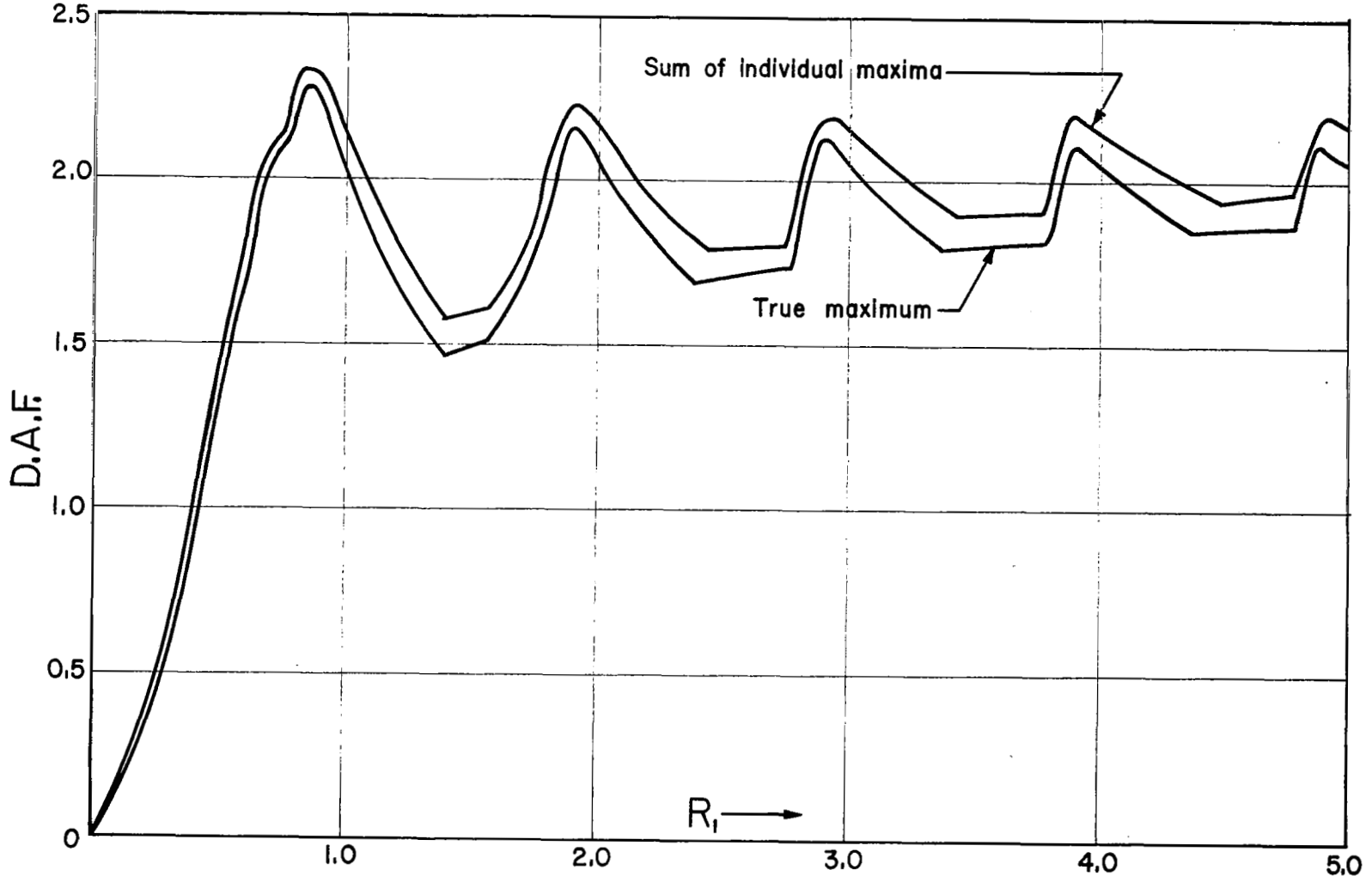

FIGURE 11. Comparison of D.A.F for simple beams obtained by two methods.

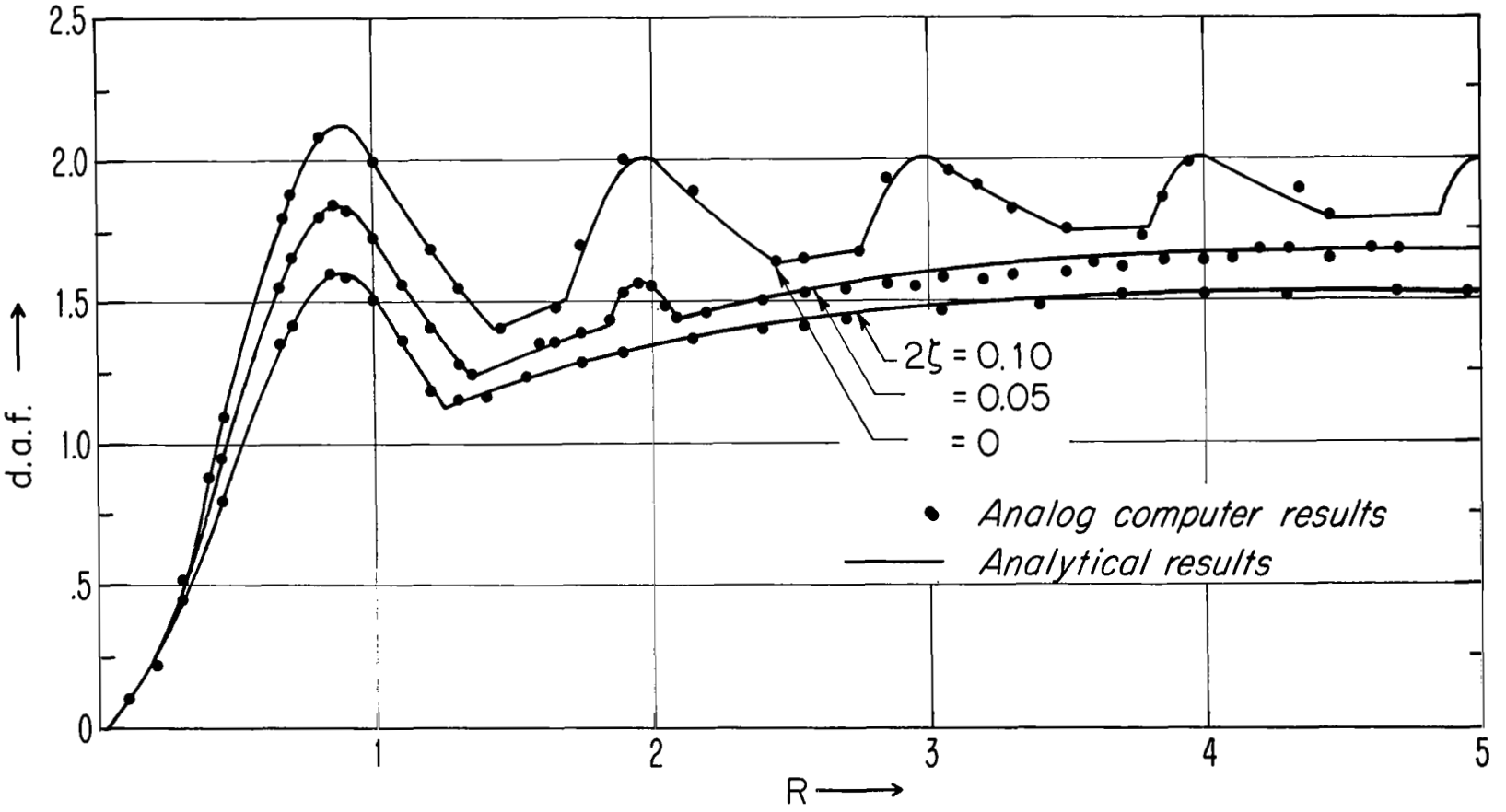

FIGURE 12. Damped d.a.f. for an N-shaped pulse.

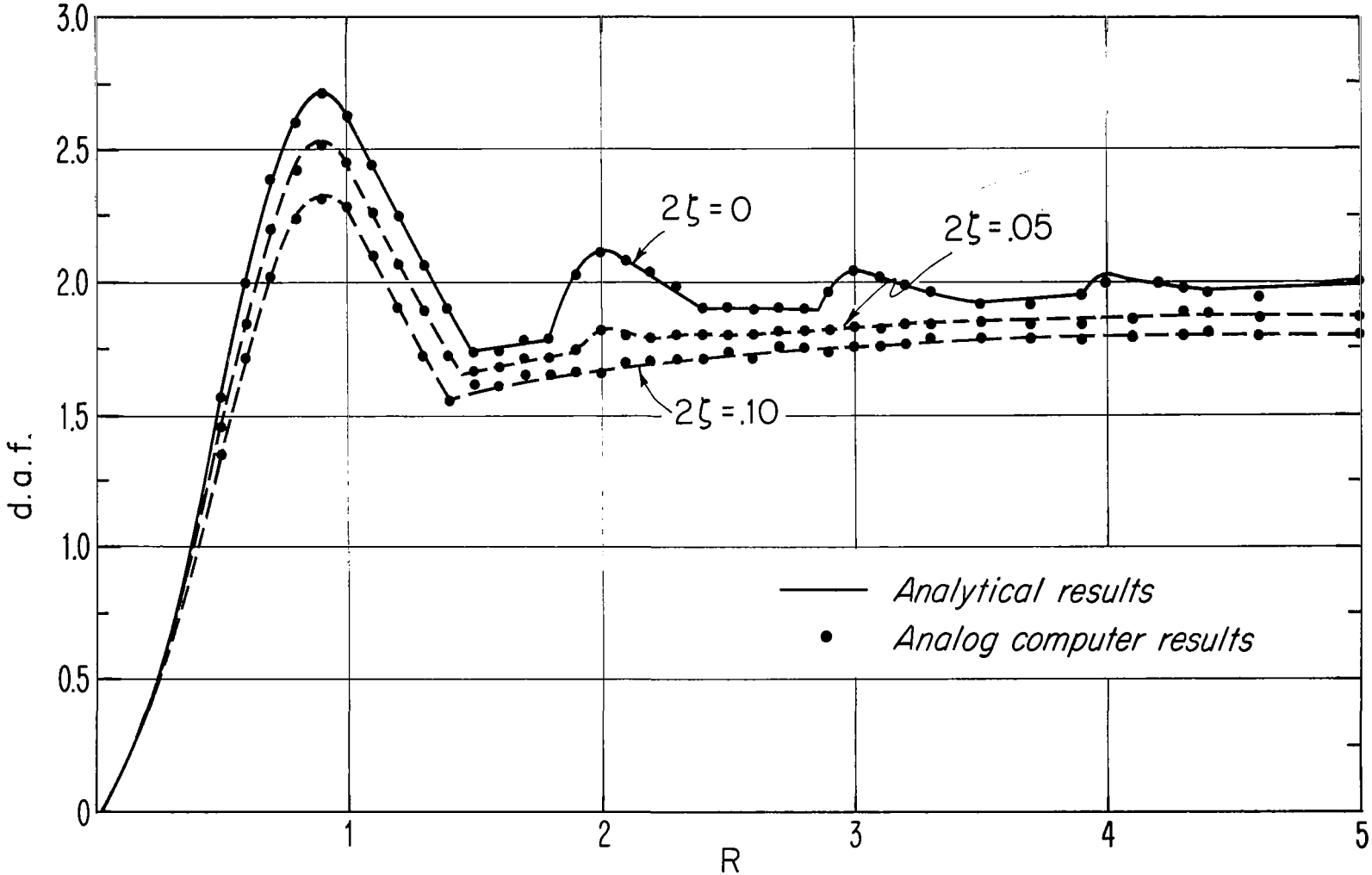

FIGURE 13. Damped d.a.f. for a half-cosine pulse.

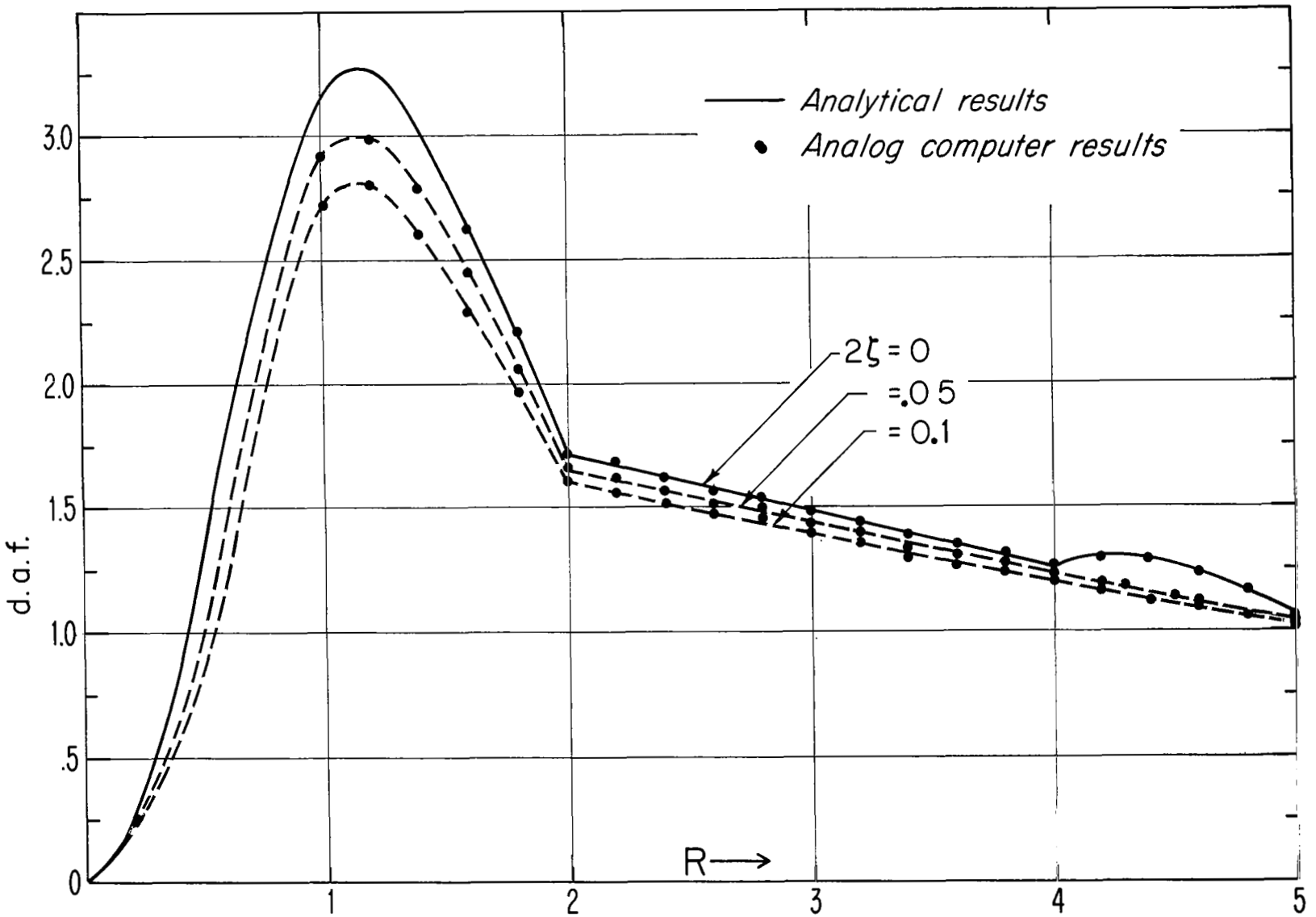

FIGURE 14. Damped d.a.f. for a sine pulse.

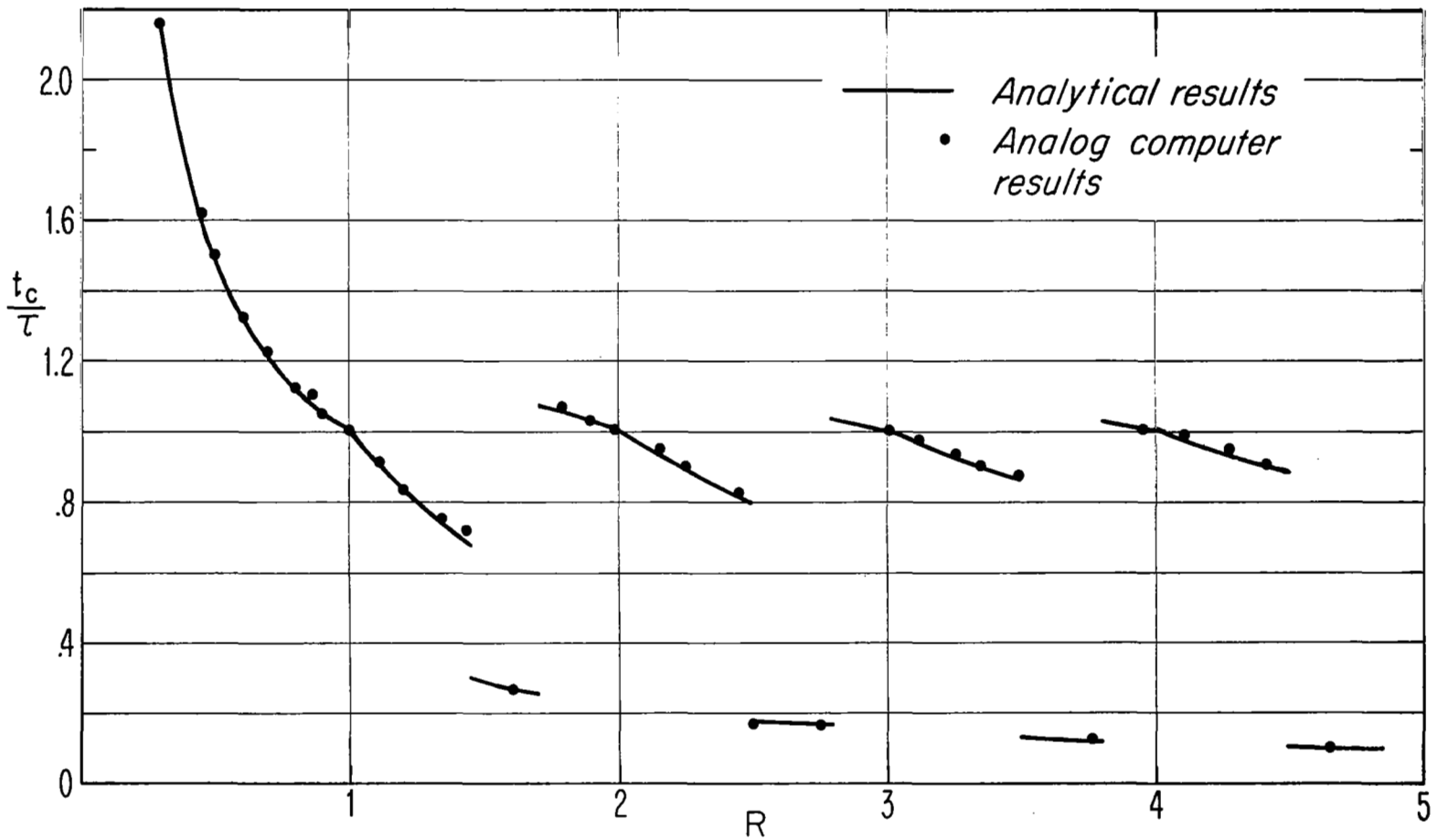

FIGURE 15. Critical time-ratio for an N-shaped pulse (no damping).

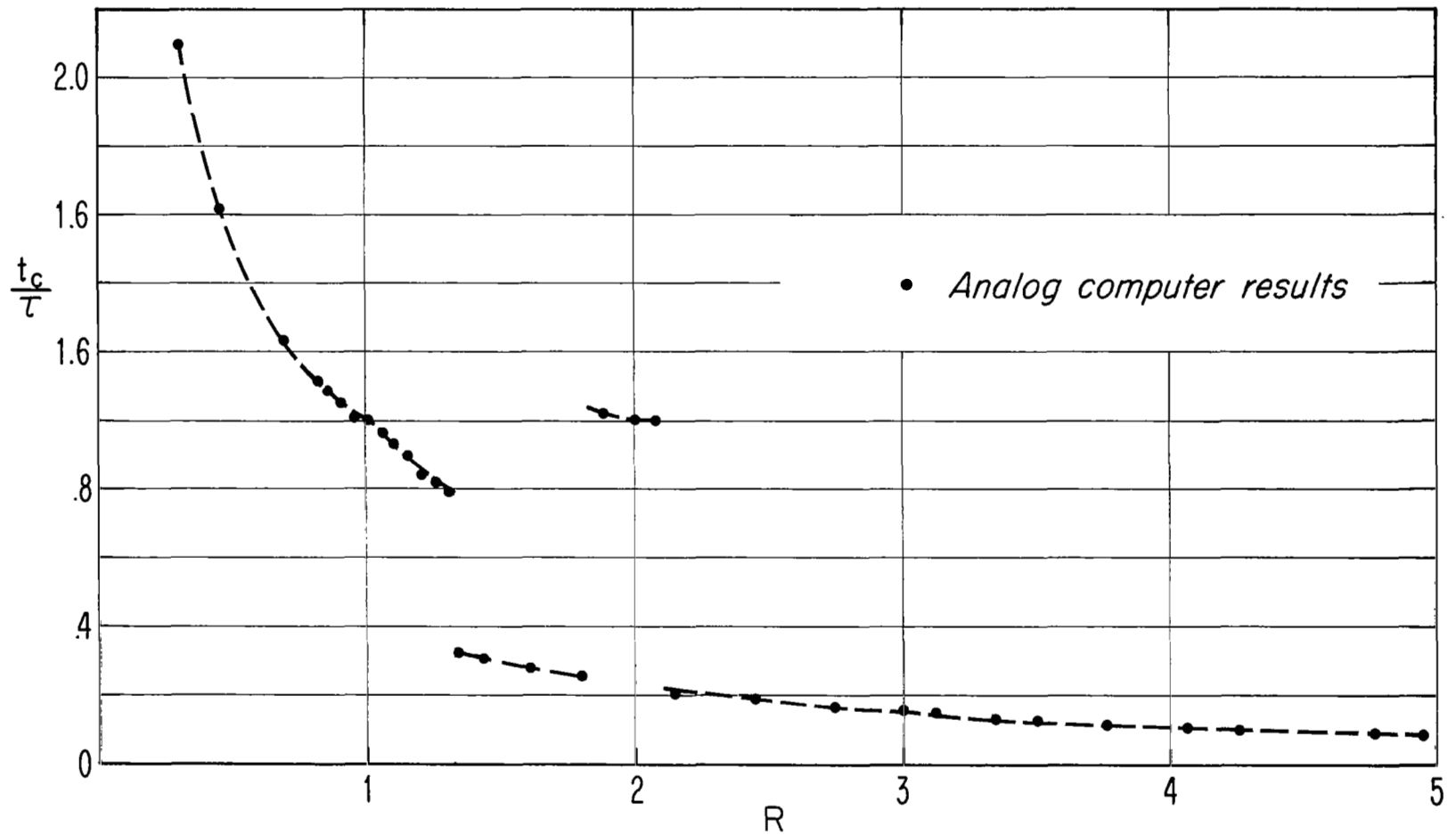

FIGURE 16. Critical time-ratio for an N-shaped pulse (with damping $\zeta = 0.025$).

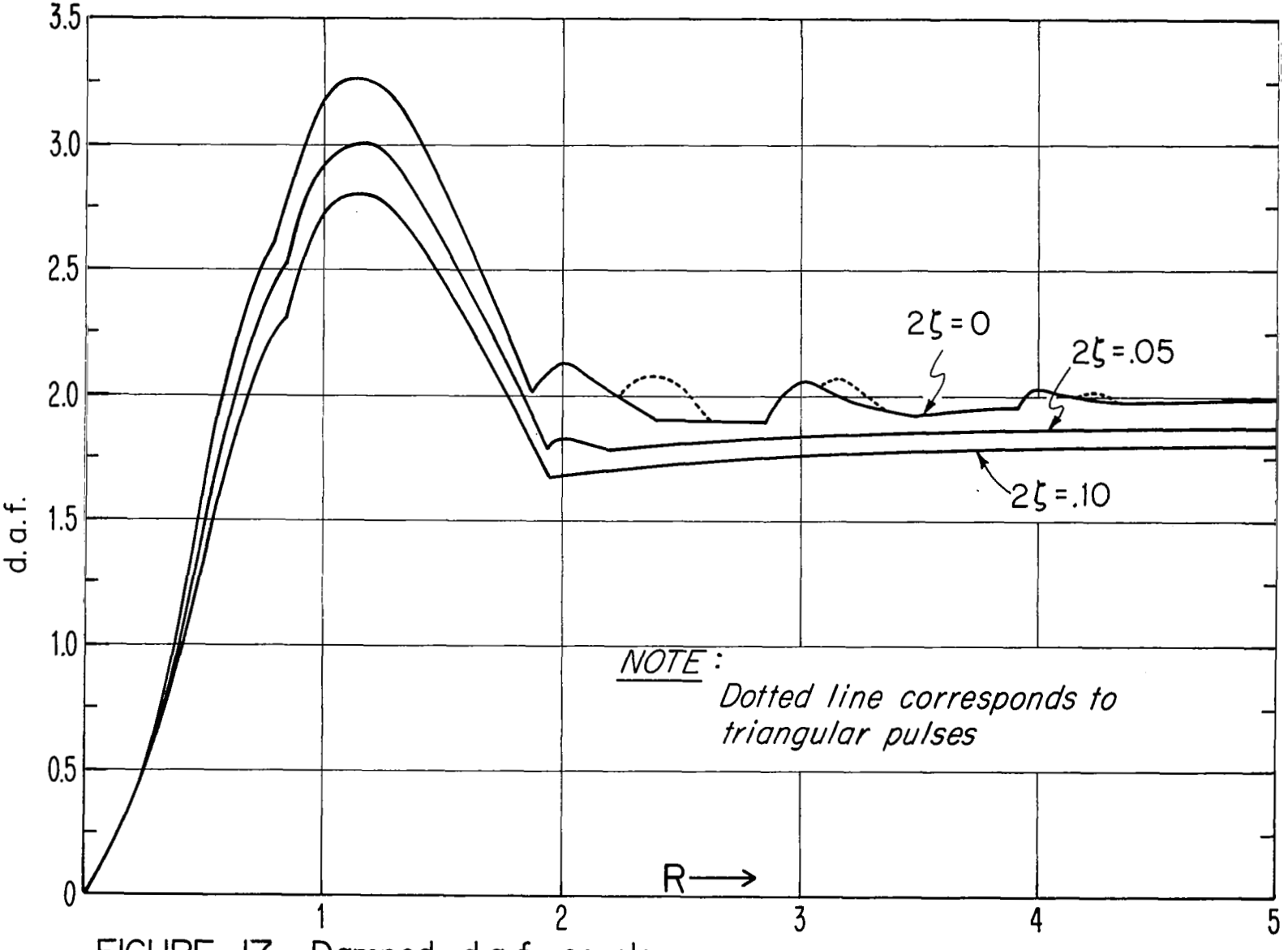

FIGURE 17. Damped d.a.f. envelope.

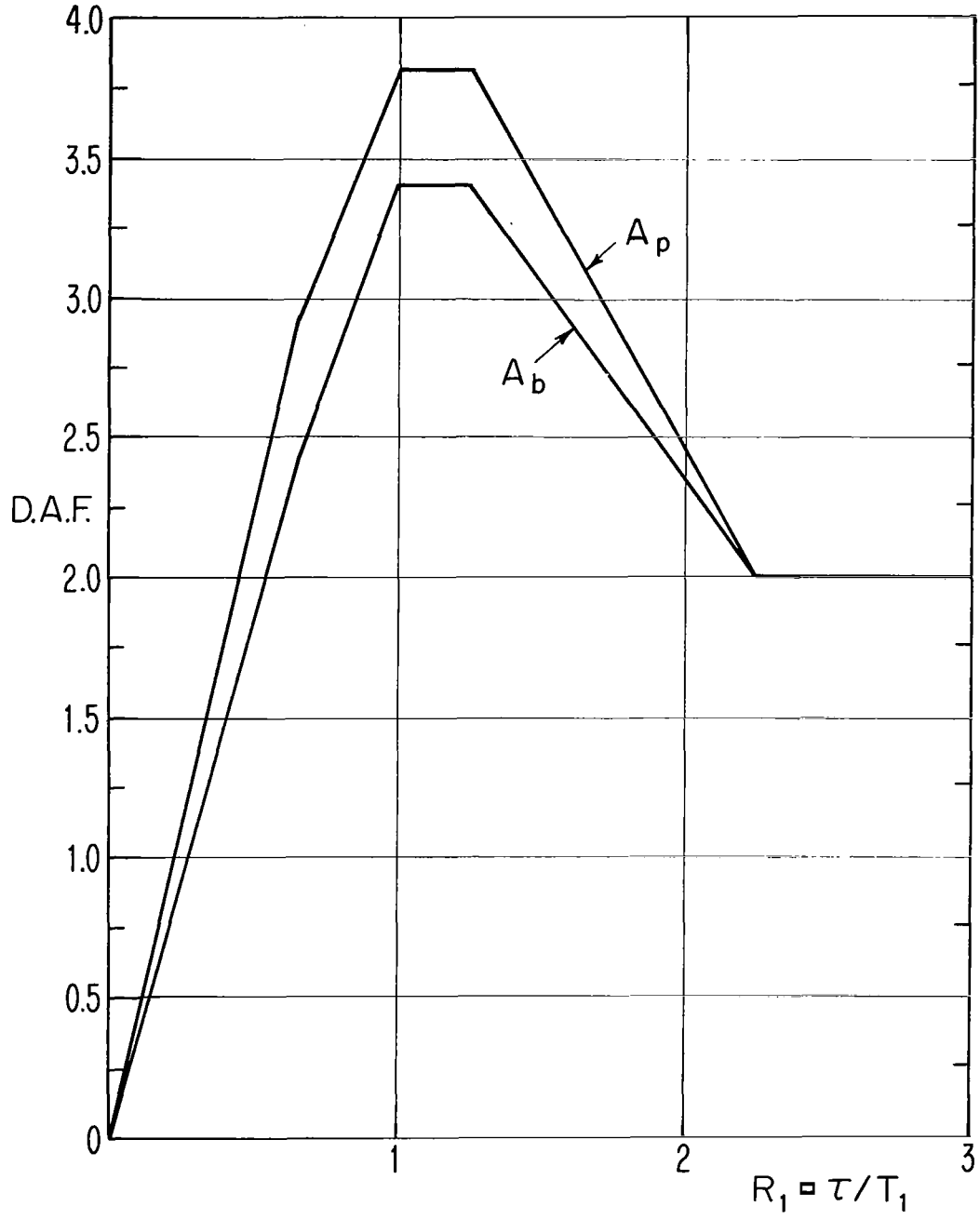

FIGURE 18. Simplified D.A.F. envelopes for sonic booms.

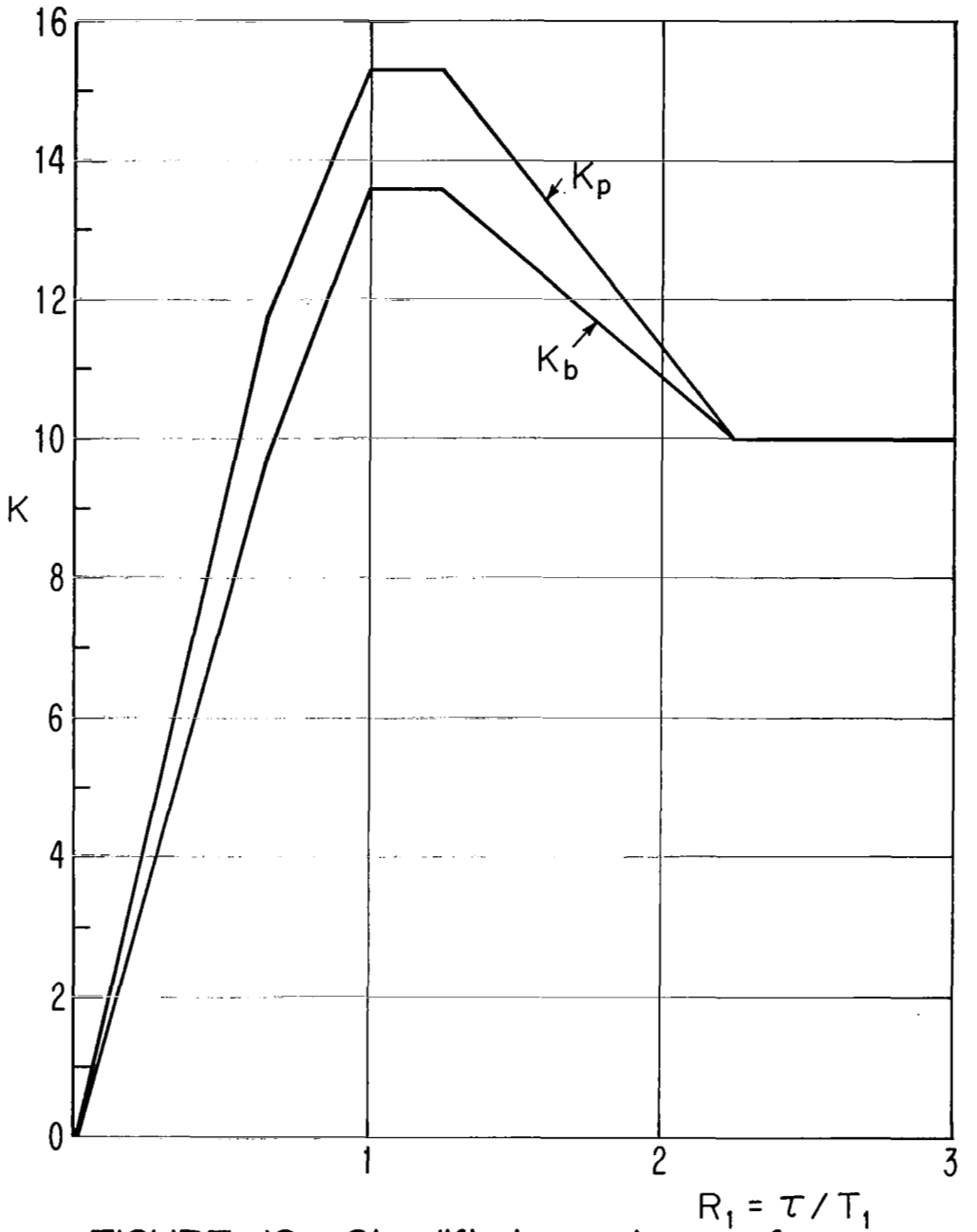

FIGURE 19. Simplified envelopes for dynamic moment coefficients.

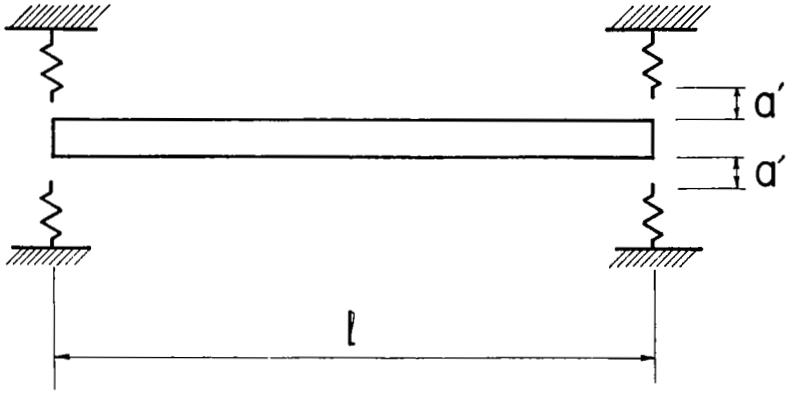

FIGURE 20. Initial state of a rattling beam.

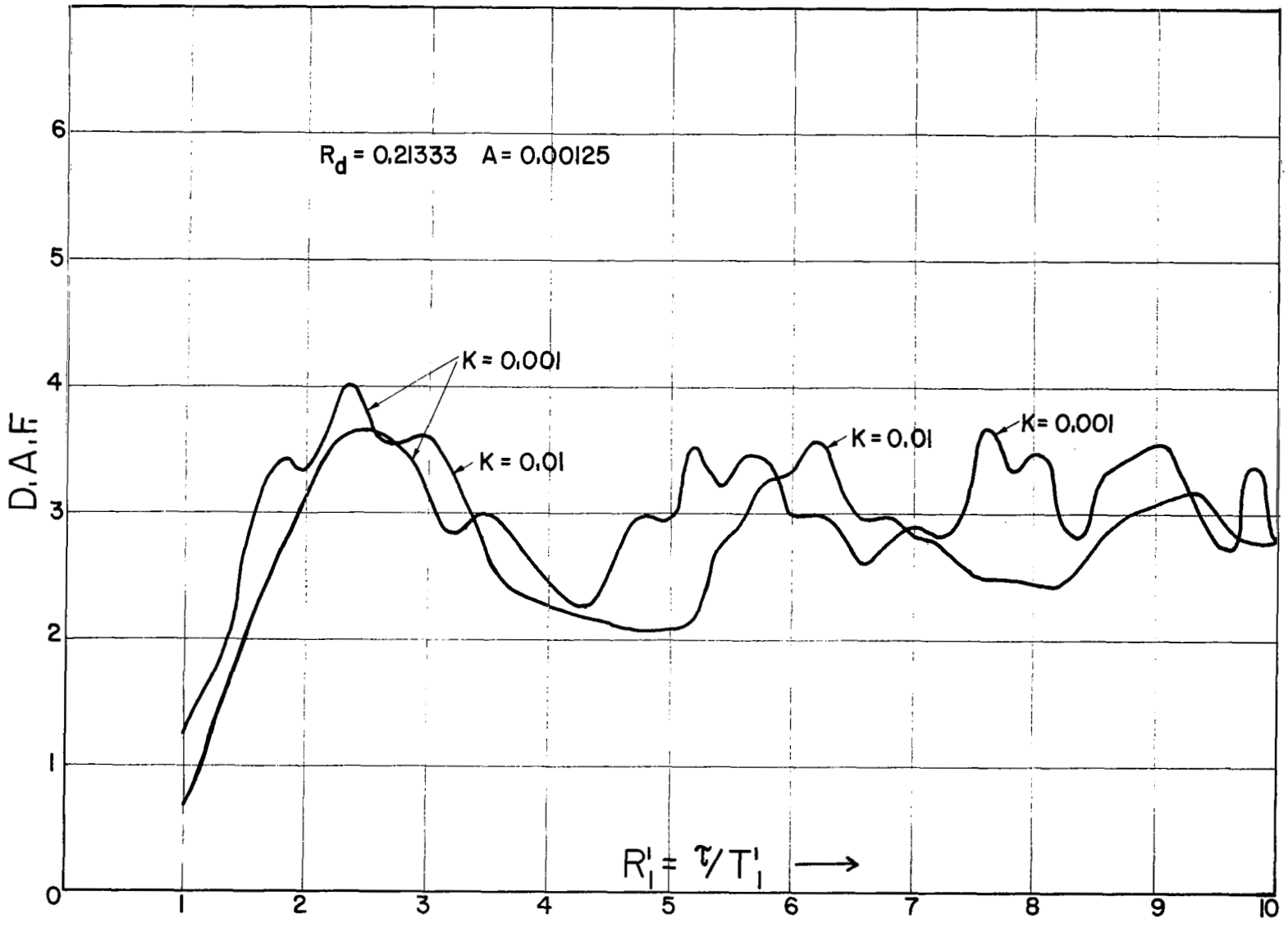

FIGURE 21. D.A.F. for center moment of a rattling beam.

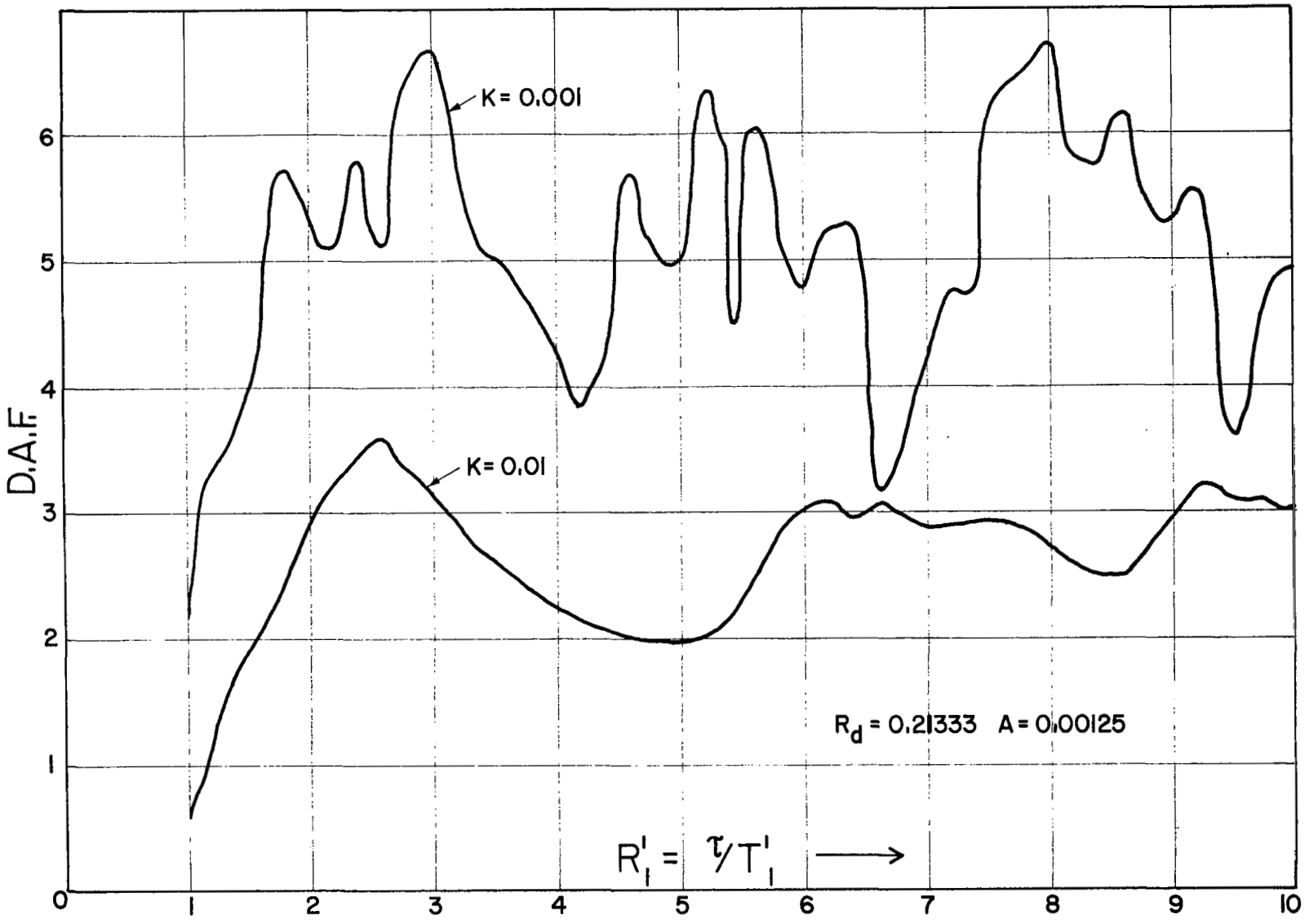

FIGURE 22. D.A.F for end-shear of a rattling beam.

NATIONAL AERONAUTICS AND SPACE ADMINISTRATION
WASHINGTON, D. C. 20546

OFFICIAL BUSINESS

FIRST CLASS MAIL

POSTAGE AND FEES PAID
NATIONAL AERONAUTICS AI
SPACE ADMINISTRATION

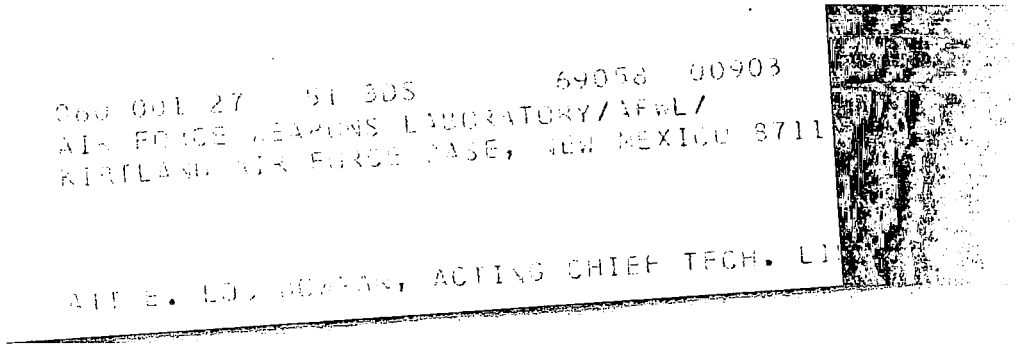

POSTMASTER: If Undeliverable (Section 15 Postal Manual) Do Not Ret

"The aeronautical and space activities of the United States shall be conducted so as to contribute . . . to the expansion of human knowledge of phenomena in the atmosphere and space. The Administration shall provide for the widest practicable and appropriate dissemination of information concerning its activities and the results thereof."

—NATIONAL AERONAUTICS AND SPACE ACT OF 1958

NASA SCIENTIFIC AND TECHNICAL PUBLICATIONS

TECHNICAL REPORTS: Scientific and technical information considered important, complete, and a lasting contribution to existing knowledge.

TECHNICAL NOTES: Information less broad in scope but nevertheless of importance as a contribution to existing knowledge.

TECHNICAL MEMORANDUMS: Information receiving limited distribution because of preliminary data, security classification, or other reasons.

CONTRACTOR REPORTS: Scientific and technical information generated under a NASA contract or grant and considered an important contribution to existing knowledge.

TECHNICAL TRANSLATIONS: Information published in a foreign language considered to merit NASA distribution in English.

SPECIAL PUBLICATIONS: Information derived from or of value to NASA activities. Publications include conference proceedings, monographs, data compilations, handbooks, sourcebooks, and special bibliographies.

TECHNOLOGY UTILIZATION PUBLICATIONS: Information on technology used by NASA that may be of particular interest in commercial and other non-aerospace applications. Publications include Tech Briefs, Technology Utilization Reports and Notes, and Technology Surveys.

Details on the availability of these publications may be obtained from:

SCIENTIFIC AND TECHNICAL INFORMATION DIVISION

NATIONAL AERONAUTICS AND SPACE ADMINISTRATION

Washington, D.C. 20546